Potential Treatment of Parkinson's Disease, Using Last-Generation Carbon Nanotubes: A Bimolecular In-Silico Study

Ehsan Alimohammadi
Kermanshah University of Medical Sciences
Arash Nikzad
University of British Columbia
Mohamad Khedri
Amirkabir University of Technology Department of Chemical Engineering
Milad Rezaeian
Shaheed Beheshti University of Medical Sciences
Ahmad Miri Jahromi
Amirkabir University of Technology Department of Petroleum Engineering
Nima Rezaei (rezaei_nima@tums.ac.i)
https://orcid.org/0000-0002-3836-1827
Reza Maleki
Sharif University of Technology

Research article

Keywords: Parkinson's Disease, Amyloid Formation, α-Synuclein, Nanotube, Molecular Dynamics

Posted Date: July 23rd, 2020

DOI: https://doi.org/10.21203/rs.3.rs-45640/v1

Potential Treatment of Parkinson's Disease, Using Last-Generation Carbon Nanotubes: a Bimolecular In-Silico Study

Ehsan Alimohammadi[1†], Arash Nikzad[2†], Mohamad Khedri[3], Milad Rezaian[4], Ahmad Miri Jahromi[5], Nima Rezaei[6,7,8*], Reza Maleki[9*]

[1] *Neurosurgery Department, Kermanshah University of Medical Sciences, Kermanshah, Iran*

[2] *Department of Mechanical Engineering, University of British Columbia, 2054-6250 Applied Science Lane, Vancouver, BC V6T1Z4, Canada*

[3] *Department of Chemical Engineering, Amirkabir University of Technology (Tehran Polytechnic), 424 Hafez Avenue, Tehran, 1591634311, Iran*

[4] *School of Medicine, Shahid Beheshti University of Medical Sciences, 19839-63113 Tehran, Iran*

[5] *Department of Petroleum Engineering, Amirkabir University of Technology (Tehran Polytechnic), 424 Hafez Avenue, Tehran, 1591634311, Iran*

[6] *Research Center for Immunodeficiencies, Pediatrics Center of Excellence, Children's Medical Center, Tehran University of Medical Sciences, Tehran, Iran*

[7] *Network of Immunity in Infection, Malignancy and Autoimmunity (NIIMA), Universal Scientific Education and Research Network (USERN), Tehran, Iran*

[8] *Department of Immunology, School of Medicine, Tehran University of Medical Sciences, Tehran, Iran*

[9] *Department of Chemical Engineering, Sharif University of Technology, Tehran, Iran*

†These authors have contributed equally to this work

[*] Corresponding Author: Prof. Nima Rezaei *rezaei_nima@tums.ac.ir* and Dr. Reza Maleki

Abstract

Background: Parkinson's disease (PD) is one of the most common neurodegenerative disorders. One of the underlying mechanisms of the disease is the accumulation of α-synuclein protein aggregates, including amyloids and Lewy bodies in the brain, resulting in the death of dopaminergic cells in the substantia nigra. The current treatments for PD are mainly focused on replacing dopamine. However, if these medications are stopped, the severity of PD will increase. Moreover, the drugs used for the treatment of PD are associated with considerable side effects and dietary restrictions. Therefore, necessary studies to develop more effective medications for PD seem to be indispensable. To prevent the progression of PD, avoiding the development of α-synuclein amyloids could be proposed.

Methods: In this study, the effects of three last-generation nanotube-based structures on α-synuclein amyloid formation were investigated for the first time employing Molecular Dynamics (MD) simulation tools. Molecular dynamics provide a deep insight into atomic interactions and can well study α-synuclein amyloid formation at the atomic and molecular scales.

Results: The molecular study results indicated that all of the nanotubes studied in this work, had strong energy interactions with α-synuclein. Therefore, nanotubes using phosphorus, nitrogen and boron dopants, have great potential to prevent α-synuclein amyloid formation. Among these nanotubes, phosphorus-doped carbon nanotube (P-CNT) has the most substantial interactions with α-synuclein. The P-CNT caused more hydrogen bonds to be formed between water and α-synuclein molecules. This phenomenon leads to a decrease in the compactness, stability, and contact area of α-synuclein proteins, which results in considerable changes in the secondary structure of α-synuclein.

Conclusions: Doping nanotubes especially P-CNT could be very effective for preventing the α-synuclein amyloid formation and hence, halting the progression of PD. This molecular study paves the way for the use of the Doping nanotubes in the treatment of PD. These structures are highly tunable and flexible. Therefore, the results of this work can be developed to computational, experimental and clinical levels.

Keywords: Parkinson's Disease, Amyloid Formation, α-Synuclein, Nanotube, Molecular Dynamics

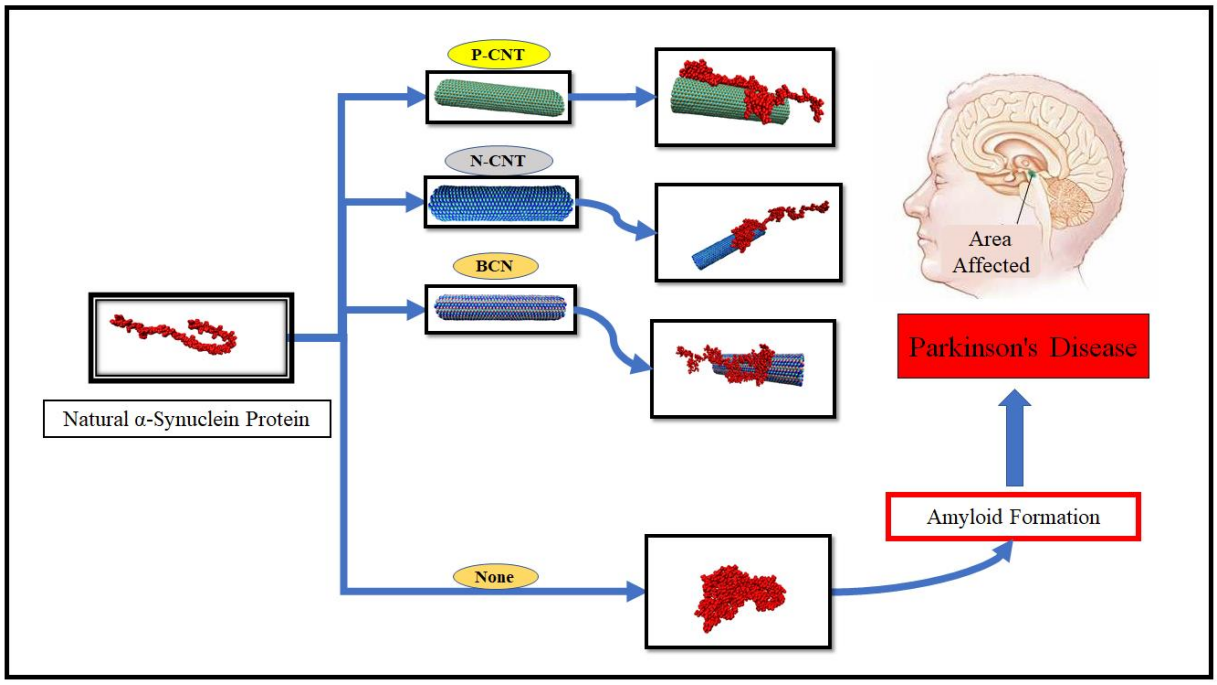
P-CNT
N-CNT
BCN
None
Natural α-Synuclein Protein
Area Affected
Parkinson's Disease
Amyloid Formation

1. Introduction

A global concern of great morbidity, neurodegenerative disorders of the central nervous system (CNS) such as PD and Alzheimer's disease have gained substantial attention in recent years. A backward glance through the extensive scientific work conducted so far reveals that much remains to be disclosed about the etiology, diagnosis, and treatment of such disorders. The loss of dopaminergic cells within an area of the basal ganglia called the substantia nigra, and the resultant imbalance between the dopaminergic and cholinergic systems, lead to the pathognomonic signs and symptoms of PD [1],[2]. The cardinal motor manifestations of PD include bradykinesia, tremor, rigidity, and postural instability. Conventional medications administered for the treatment of PD have minimized the severity of such symptoms and substantially enhanced the patients' quality of life.[3] Dopamine replacement therapies have long been the mainstay of treatment along with other drugs, including amantadine, selegiline, and biperiden. Although these medications slow down the course of the disease, they cannot terminate the progression of PD. [4]–[6]On the other hand, stopping their administration will result in the recurrence of symptoms with escalated severity. As the course of the disease progresses, more diverse symptoms such as cognitive impairment, psychological disorders, autonomic dysfunction, tend to appear, indicating the existence of a more ubiquitous underlying pathophysiology, and necessitating the development of novel, more effective treatments [7]–[9].

Microscopic examination of autopsy specimens taken from the brain of dead patients with PD reveals the presence of specific protein aggregates within the brain tissue, called amyloid fibrils and Lewy bodies. These aggregates are dense protein polymers consisting of α-synuclein monomers. The α-synuclein is a protein of the synuclein family consisting of 140 amino acids, which in its natural state, carries out critical intracellular functions. It is believed that this protein has critical roles in the neuronal signaling, from the synthesis and transport to the secretion and recycling of neurotransmitters. Under certain pathologic circumstances, this protein loses its natural folding [10]. The misfolded α-synuclein proteins tend to aggregate, giving rise to oligomers, protofibrils, amyloid fibrils, and Lewy bodies, consecutively. These cytotoxic agents can propagate between neurons in various ways such as exosomes, receptor-mediated transport, endocytosis, synaptic transmission, direct penetration, and hence, gradually spread through the

brain [11], [12]. Furthermore, it has been indicated that misfolded α-synuclein proteins, as the primary culprit for the vicious cascade, can induce the misfolding of natural α-synuclein proteins by direct contact, escalating the spread of the disease (**Figure 1**). Therefore, it can be concluded that preventing α-synuclein proteins from becoming misfolded, and the resultant inhibition of amyloid and Lewy body formation could be regarded as a propitious measure for the prevention and treatment of PD. [13]–[19]

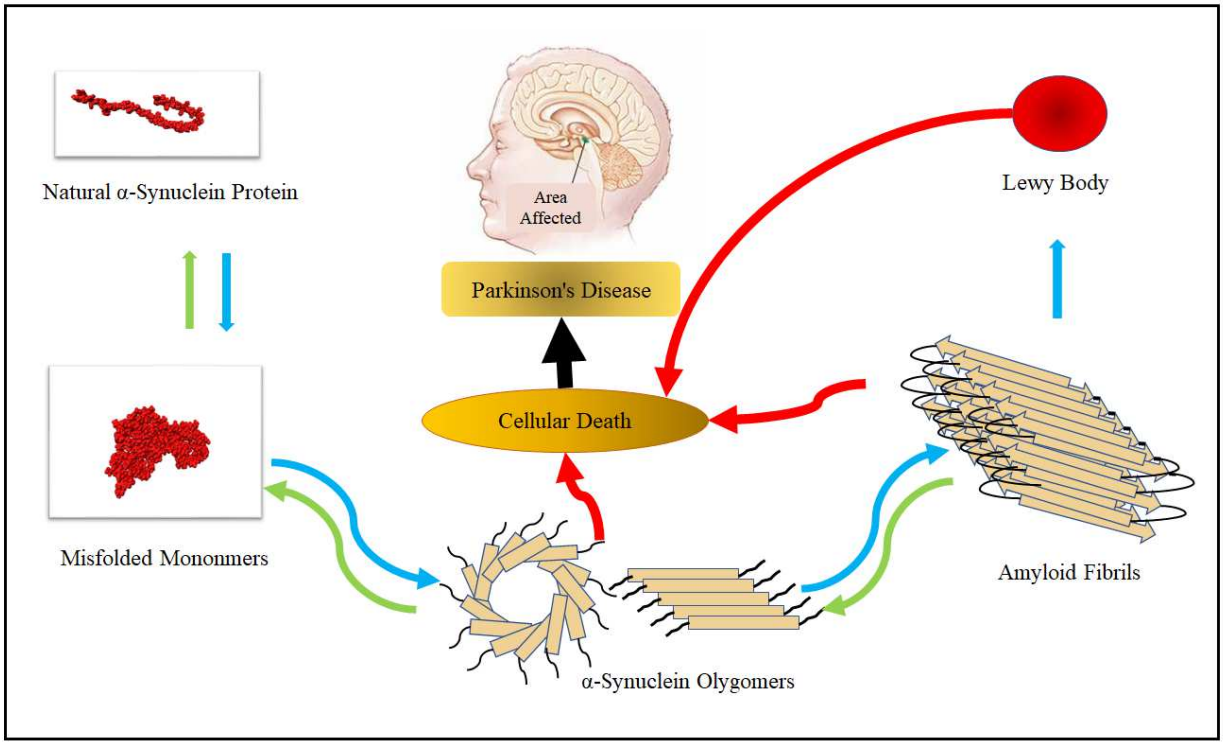

Figure 1 - Amyloid fibrillation process and its role in the formation of PD

To date, many studies have been centered around the prevention of α-synuclein amyloid formation.[20] In these studies , specific biochemical agents have been applied to establish the objective. Among these agents, there have been several nanoparticles, including gold nanoparticles, superparamagnetic iron oxide nanoparticles (SPIONs), quantum dots (QDs), graphene and nanotube derivatives [21]–[23]; these agents can affect the process of amyloid formation in different ways. By the strong interactions they make with proteins and the abundant hydrogen bonds they induce between proteins and water molecules, nanoparticles can inhibit

the formation of specific spatial configuration required for amyloid precursors to aggregate. Such interactions also decrease the contact surface of proteins, which would reduce their chance of polymerization. Furthermore, some nanoparticles have been shown to decrease amyloid precursors' molecular compactness, a feature ordinarily required for amyloid formation. Such impacts have progressively motivated the development and application of more appropriate nanoparticles as potential treatment options for amyloid-based disorders [24]–[27].

Carbon nanotubes (CNTs) are hollow cylindrical structures consisting of carbon atoms arranged in single or multi-walled configurations. Having metallic and quasi-conductive properties, CNTs' specific features, including relatively large surface areas, high permeability, and exceptional mechanical and thermal stability, have brought them about a wide variety of utilities. Since their discovery in the 1990s, CNTs have been increasingly applied in nanomedicine for various diagnostic and therapeutic purposes [28], [29]. They have been used in drug delivery systems, tissue engineering, the diagnosis and treatment of malignancies, and biosensors. With the intent to implement CNTs in such diverse applications, making structural and chemical modifications to this carbon allotrope as to be adjusted for different utilities seem inevitable. This fact has led to the development of successive new generations of CNTs. Second-generation CNTs were synthesized by chemical functionalization. Chemically functionalized CNTs were shown to make better interactions with bio-system components and presented more favorable solubility properties. However, despite their vast utilities, second-generation CNTs seemed to be technically flawed for some novel applications. Ultimately, the last-generation CNTs or -doped CNTs were developed as a certain proportion of carbon atoms were replaced by other elements like nitrogen, bromine, and phosphorous [30], [31].

This study, for the first time, investigated the impacts of three types of last-generation CNTs on α-synuclein amyloid formation by molecular dynamics simulation tools. These CNTs include phosphorus-doped carbon nanotube (P-CNT), nitrogen-doped carbon nanotube (N-CNT), and nanotube co-duped with bromine and nitrogen (BCN). In this study, the functionality of nanoparticles, and various parameters involved in their interactions with α-synuclein proteins have been compared. In order to validate the model employed in this study, the results initially compared with Mohammad-beigi *et al.* [32]. The remainder of the paper is organized into three

sections: section two describes the method that was used in this study, results are presented in section three, and the last section concludes the paper.

2. Methods

2.1. Molecular Dynamics Simulation

Today, with the advancement of computer technology, special attention is paid to calculate the properties of materials using the structure of their constituent particles via simulation. Molecular dynamics (MD) is a method for analyzing the physical motion of atoms and molecules. In the molecular dynamics simulation, the "real" dynamic behavior of the system is calculated. By applying Newton's motion equations, a set of atomic positions is obtained sequentially. MD is an estimation method, in the sense that the state of the system at any future time can be predicted from its current state [33]. A large number of atoms in molecular systems make it impossible to perform analytical calculations to obtain the properties of these complex systems. Therefore, the properties of molecular systems are calculated, using numerical methods.

MD produces information at the microscopic level, such as position and speed of atoms, and the data are converted to macroscopic values such as pressure, and energy, using statistical mechanics. MD and statistical mechanics link microscopic properties and observable macroscopic quantities. In molecular dynamics simulations, changes in the system over time are made using Newton's second law. MD simulation applies Newton's equations of motion in a specific manner to predict the upcoming moments based on current conditions. Initially, the characteristic of atoms and their physical properties are obtained. Then, for every atom in the system, a neighbor list consist of those atoms within the force range are created, which changes at each step. Finally, the applied force on atoms is calculated.

Newton's motion equation is function of the position of the atom (r_i) in a N atomic system:

$$\mathrm{m_i}\frac{d^2 r_i}{dt^2} = F_i \quad , \qquad i = 1, \dots, N \tag{1}$$

m_i is the mass of the atom, and F_i is the force applied by the rest of the atoms to the atom i. MD simulation, in fact, specifies the trajectory of molecules. The force acting on atom i in an N atom system, is derived from potential function (r) :

$$F_i = -\frac{\partial u}{\partial r_i} \quad , \qquad i = 1, \dots, N \tag{2}$$

It is possible to study the temporal evolution of the simulation system by having initial velocities and positions. How to change the position, velocity, and acceleration of particles is obtained over time by integrating Newton's motion equations. By simulating molecular dynamics, quantities based on the position and velocity of atoms can be obtained. The measurement of physical quantities in molecular dynamics is done by averaging those quantities over the simulation time [34], [35].

2.2. Simulation method

To simulate the molecular structure of carbon CNTs, the Nanotube_Modeler_1.7.9 was used [36]. Using Avogadro software in this simulation, carbon CNTs were replaced with bromine and nitrogen, nitrogen, and phosphorus atoms to reach BCN, N-CNT, and P-CNT molecular structures, respectively. The molecular structure of α-synuclein (1XQ8) was extracted from[37]. Besides, the molecular structures of the carbon CNTs doped with bromine, nitrogen, and phosphorus were optimized by Gaussian 09 software [38].

The topological parameters of nanoparticles and α-synuclein proteins are designed for the Optimized Potentials for Liquid Simulations (OPLS) force field [39]. The optimization was performed in 5000 time-steps, with one femtosecond, and the energy level of $100\ KJ/mol$. The NVT simulation system is coupled with the Berendsen thermostat algorithm and is balanced over 100 picoseconds at 310 K [40]. Using the Parrinello_Rahman algorithm in the NPT phase, the simulation reaches equilibrium at a pressure of 1 bar in ten nanoseconds [41] .Furthermore, applying the Linear Constraint Solver (LINCS) algorithm with h_bond and the cut off radius of 1.4 nanometers, the simulation was solved in 40 nanoseconds.

3. Validation

The molecular dynamics of graphene polyglycerol and amyloid in water were simulated by Hossein Mohammad-Beigi et al. [32]. Since the force field OPLS and the simulation method LINCS in this article are very similar to Hossein Mohammad-Beigi et al. [32], the results of the repeated VDW energy in the same condition were compared to validate the results (**Figure 2**). This figure shows the results of this study, and Hossein Mohammad-Beigi *et al.* [32] are in agreement, which validates the results in this study.

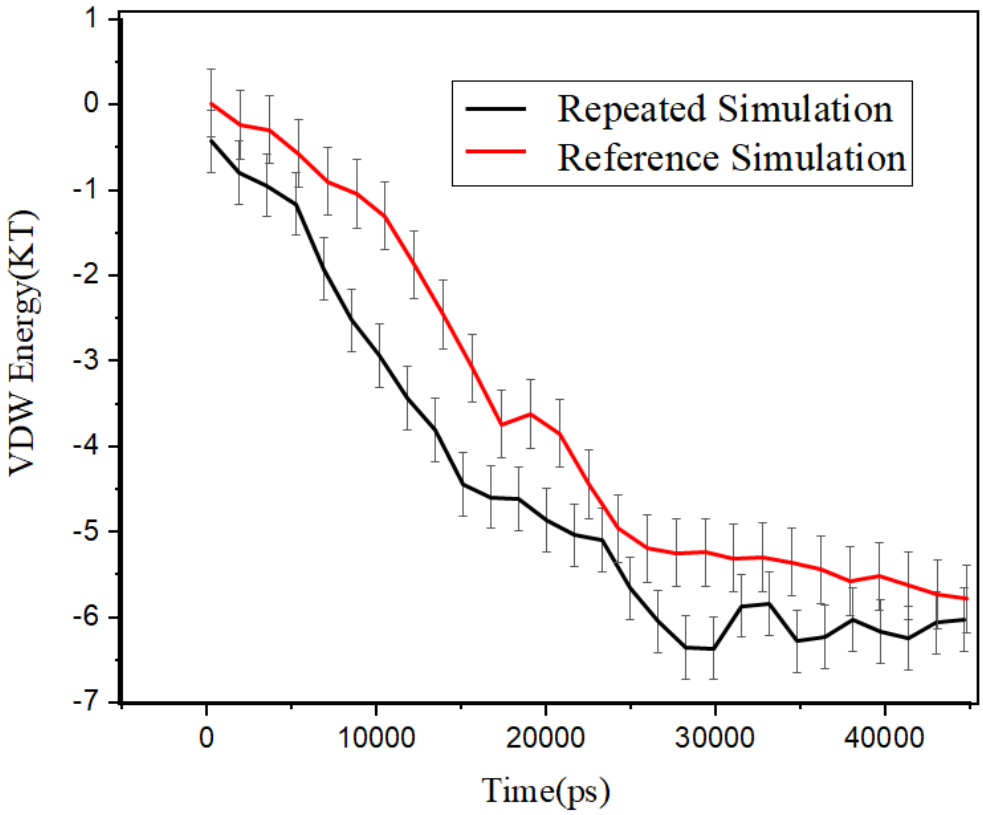

Figure 2 – VDW energy in this study and [32] to validate the results

4. Results

Figures 3a to **3d** show α-synuclein in the simulation with BCN, P-CNT, and N-CNT after 40 nanoseconds, while **Figure 3e** shows the folded α-synuclein. The compression of the protein particles in this figure is quite apparent. This folding in α-synuclein causes favorable conditions for amyloid fibrillation. The results of α-synuclein simulation in the presence of nanoparticles clearly show their positive effect in preventing the formation of α-synuclein structure. Specifically, it is shown that P-CNT is the most effective nanoparticle to prevent amyloid fibrillation.

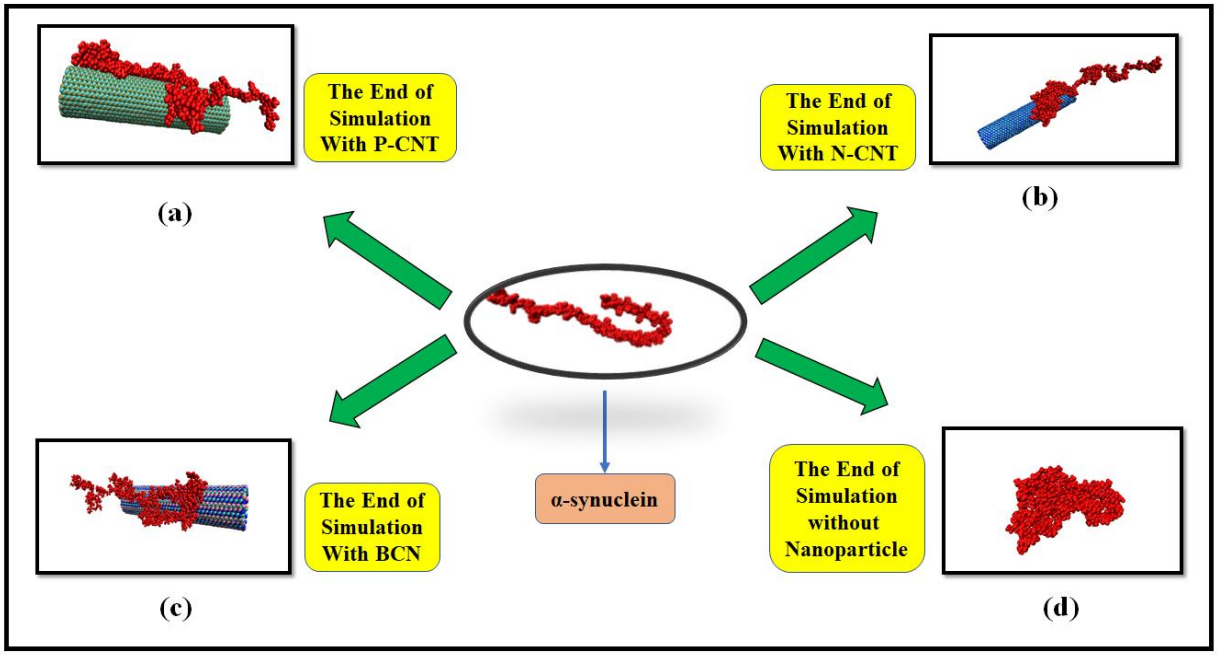

Figure 3 – Results of α-synuclein simulation after 40 nanoseconds with a) P-CNT b) N-CNT c) BCN d) Without Nano Particle

4.1 . Interactions between nanoparticles and α-synuclein and its effect on amyloid fibrillation

Van der Walls (VDW) and electrostatic interactions are two examples of intermolecular interactions. The greater the electrostatic and vandal interaction of α-synuclein and

nanoparticles, the lower the interaction between α-synuclein particles, and consequently, the alteration in the α-synuclein chain. The more significant electrostatic and VDW attraction between nanoparticles and α-synuclein proteins causes lower stimulation energy levels. The lower the simulation energy level, the greater the effect of nanoparticles on preventing amyloid fibrillation. Energy analysis is one of the most critical analyzes for the study of intermolecular interactions. By analyzing the energy, it is possible to study the VDW and electrostatic bonds during the simulation [42]–[44]. Eq. 3 and Eq.4 indicate the Lenard-Jones and Colum's law to calculate the VDW and the electrostatic interactions energy.

$$\mathrm{V}_{\mathrm{vdw}} = 4\epsilon\,[\left(\frac{\sigma}{r}\right)^{12} - \left(\frac{\sigma}{r}\right)^{6}] \tag{3}$$

$$U_{\{E\}}(r) = (4\pi\epsilon)^{-1}\frac{q_i q_j}{r_{ij}^2} \tag{4}$$

Figure 4 presents the energy diagrams from VDW and electrostatic bonds to simulate different nanoparticles and α-synuclein proteins versus the simulation time. In α-synuclein simulations, in the presence of BCN, P-CNT and N-CNT, the energy generated by the electrostatic bonds between the nanoparticle and the α-synuclein protein are approximately equal to zero. Small electrostatic bonds have matched the lines of energy, VDW (black lines), and total energy simulation (blue lines). In all of the simulations, the energy from the VDW bonds overcomes the energy from the electrostatic bonds. The VDW scale indicates the more significant effect of the VDW attraction on preventing amyloid fibrillation. It is shown that in all four simulations, as the simulation time increases, the energy level decreases due to higher interaction between nanoparticles and α-synuclein proteins. This figure shows that a significant increase in the attraction between nanoparticles and α-synuclein molecules occurs between 30 and 40 nanoseconds. The total energy level of all four simulations is negative that shows the gravitational pull between the nanoparticles and the α-synuclein molecule. The continuous decrease in energy during the simulation and the negation of total energy in all four simulations indicate the optimal effect of nanoparticles in preventing amyloid fibrillation.

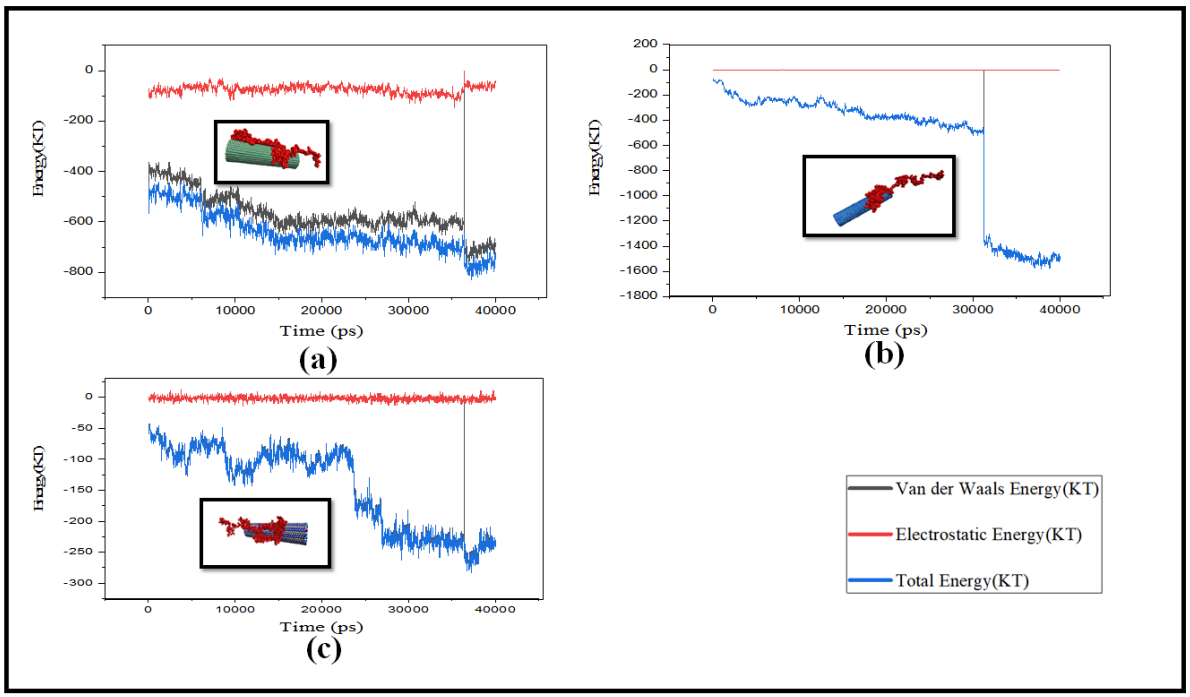

Figure 4 - Nanoparticle simulation energy diagrams a) P-CNT b)N-CNT c) BCN and α-synuclein in protein over 40 nanoseconds

Table 1 shows the average energy generated by the VDW and electrostatic bonds over time of protein simulation in the presence of different nanoparticles. The absolute value of the total energy of VDW and electrostatics is a good indicator for comparing the level of interactions between α-synuclein protein and nanoparticles. The absolute value of energy in BCN simulation is significantly different from other simulations. Although the negative energy in this simulation indicates the attraction between nanoparticles and α-synuclein proteins, the low absolute value of energy in this simulation indicates the small effect of nanoparticles in preventing amyloid fibrillation compared to other nanoparticles. Among the other three simulations, α-synuclein simulation in the presence of P-CNT and N-CNT has the highest and lowest energy values, respectively. P-CNT and N-CNT nanoparticles have the highest interactions with α-synuclein proteins, respectively. P-CNT nanoparticles have the most significant effect on preventing amyloid fibrillation due to their high interaction with α-synuclein protein. Energy Analysis has shown that P-CNT is the best nanoparticle to prevent PD (**Table 1**).

Table 1- Average VDW, average electrostatic, and total energy of nanoparticles in 40 nanoseconds

Nanoparticle	P-CNT	N-CNT	BCN
Van der Waals Energy(KT)	-234.34	-237.94	-62.7
Electrostatic Energy(KT)	-29.9	0.001	-0.69
Total Energy(KT)	-264.39	-238.37	-63.43

4.2. Secondary structure analysis

When folding in the structure of proteins, the protein chain takes different forms due to the formation of hydrogen bonds between its particles. Different forms of protein make secondary structures during folding. The most common secondary structures are the α_helix and the β_sheet. Both structures are formed by the hydrogen bonds between the O carbons of the carbonyl group of one amino acid and the H atom of another amino acid. α-synuclein is a right spiral. Its structure is repeated every 5.4 angstroms. Since there are 3.6 amino acids in an α_helix round, every 1.5 angstroms an amino acid exists. Each group of carboxylic and amines in an α_helix has a hydrogen bond with amino acids at a distance of four, and this pattern is repeated throughout the helix, except for the four amino acids at the end. The structure of β_sheet is very elongated and wrinkled. One of the significant differences between beta and α-synuclein plates is the proximity of amino acids in this structure. Therefore, β_sheet has little flexibility. The interdisciplinary hydrogen bonds formed between the CO groups of a beta-strand and the NH adjacent beta strings stabilize the β_sheet and cause these plates to have a zigzag appearance.

However, α_helix and β_sheet are not the only secondary structures. Other secondary structures include Coil, B-Bridge, Bend, and Turn [45]–[47]. α-synuclein protein naturally lacks secondary structures and is an integral part of proteins. α-synuclein protein has 140 amino acid groups in its molecular structure. Amino acids in this protein are divided into three categories. In the first group (amino acids 1 to 60), there are conditions for the formation of α-synuclein structure. In the second step (amino acids 61-95), the conditions for the formation of beta plates are created. Nevertheless, the third group (amino acids 96-140) has acidic properties, and there is much

proline in this area. The presence of proline in this area prevents the formation of β_sheet. This area can control the formation of amyloid fibrils [48].

Amyloid fibrillation is associated with an increase in helices and β_sheet structures and a decrease in Turn, Bend, and coil structures. Therefore, the study of secondary structures created in α-synuclein protein after the simulation is a perfect indicator to compare the performance of different nanoparticles in preventing α-synuclein chain folding and amyloid fibrillation. **Figure 5** shows the secondary structures of the α-synuclein protein in the presence and absence of various nanoparticles. More details of the secondary protein structures in the presence of nanoparticles are shown in **Table 2** and **Table 3** . The presence of nanoparticles increased Turn, Bend, and coil structures, and reduced helices and β_sheet structures in α-synuclein proteins. The performance of nanoparticles has been positive in preventing protein depletion. However, the increase in Turn, Bend, and Coil structures has been the highest in protein simulation in the presence of P-CNT, N-CNT, and BCN nanoparticles.

Furthermore, helices and β_sheet structures had the most considerable reductions in protein simulations, respectively. Although BCN is effective in preventing the formation of α-synuclein oligomers, it has been less effective than other nanoparticles. P-CNT, on the other hand, is the most effective in preventing the formation of the α-synuclein oligomer. Define Secondary Structure of Proteins (DSSP) analysis has shown P-CNT to be the most effective nanoparticle to prevent amyloid fibrillation.

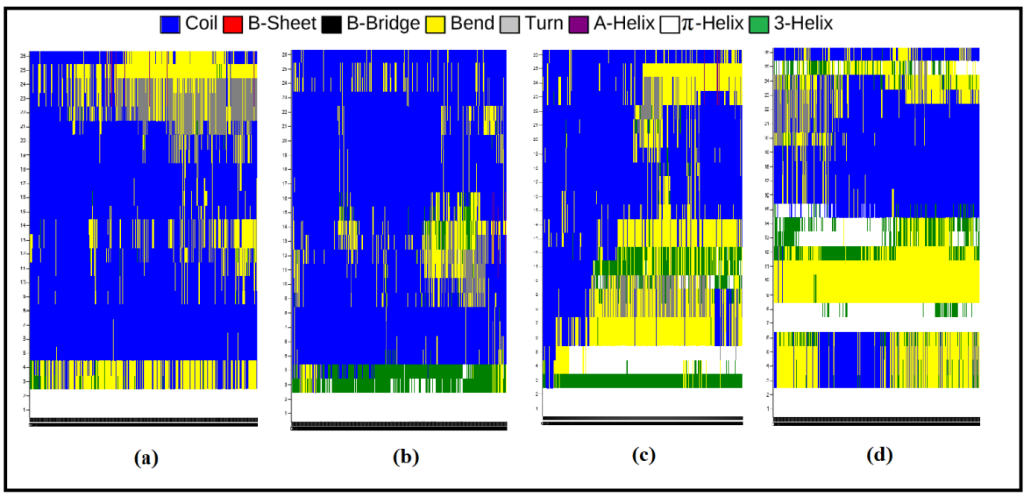

Figure 5- the secondary structure of α-synuclein in the presence of a) P-CNT b) N-CNT c) BCN d) Without Nano Particle

Table 2- The secondary structures of α-synuclein protein in the presence of nanoparticles

Nanoparticle		Structure	Coil	B-Sheet	B-Bridge	Bend	Turn
P-CNT	Total	1318328	2866010	24	10080	1127899	966802
	Average	32.95	71.65	0.0006	0.25	28.19	24.17
	Percent	0.24	0.51	0	0	0.2	0.17
N-CNT	Total	1329083	2227167	2854	111873	1808571	766245
	Average	33.22	55.67	0.07	2.79	45.21	19.15
	Percent	0.24	0.4	0	0.02	0.32	0.14
BCN	1513505	2324654	694	124253	1482734	893511	495047
	Average	37.83	58.11	0.017	3.11	37.07	22.34
	Percent	0.27	0.42	0	0.02	0.26	0.16
None	Total	1622821	1928421	81064	136748	1697853	861803
	Average	40.57	48.21	2.03	3.42	42.44	21.54
	Percent	0.29	0.34	0.01	0.02	0.3	0.15

Table 3-The secondary structures of α-synuclein protein in the presence of nanoparticles

Nanoparticle		A-Helix	5-Helix	3-Helix	Turn+Bend+Coil	Helices+B-Sheet
P-CNT	Total	341422	44965	242938	4960711	629349
	Average	8.54	1.12	6.07	124.01	15.73
	Percent	0.06	0.01	0.04	0.88	0.11
N-CNT	Total	448111	4004	231315	4801983	686284
	Average	11.2	0.1	5.78	120.05	17.16
	Percent	0.08	0	0.04	0.86	0.12
BCN	1513505	4220	275027	332334	1389252	735834
	Average	12.38	0.1	6.87	117.52	19.37
	Percent	0.09	0	0.05	0.84	0.14
None	Total	543206	106531	244514	4488077	975315
	Average	13.58	2.66	6.11	112.19	24.38
	Percent	0.1	0.02	0.04	0.79	0.17

4.3.α-synuclein protein particles contact area

Increasing the contact area between the protein particles provides favorable conditions for the interaction of the particles. As the conditions are more conducive to the interaction of the particles, the probability of amyloid fibrillation increases. Solvent Accessible Surface Area(SASA) analysis makes it possible to investigate changes in the contact area of protein particles during the simulation [49], [50]. The changes in the contact area of amyloid particles is defined by:

$$\text{Contact Area (t)} = 0.5 \times (\text{ca}_0 - ca_t) \quad (5)$$

where ca_0 and ca_t show the amount of SASA analysis at zero and at time t, respectively. Contact area variation of protein particles shows the ability of different nanoparticles to inhibit the interactions of α-synuclein protein particles. **Figure 6** shows the contact area of the α-synuclein protein in $nm \setminus S2 \setminus N$ in the presence and absence of nanoparticles. Contact area reduction in protein has a positive effect on nanoparticles in preventing protein particle interactions. After ten nanoseconds, the contact area starts changing, while small changes after ten nanoseconds

occur, which indicates a relative equilibrium in the system. The results show that the reduction in the contact area in the presence of P-CNT is higher than in other cases.

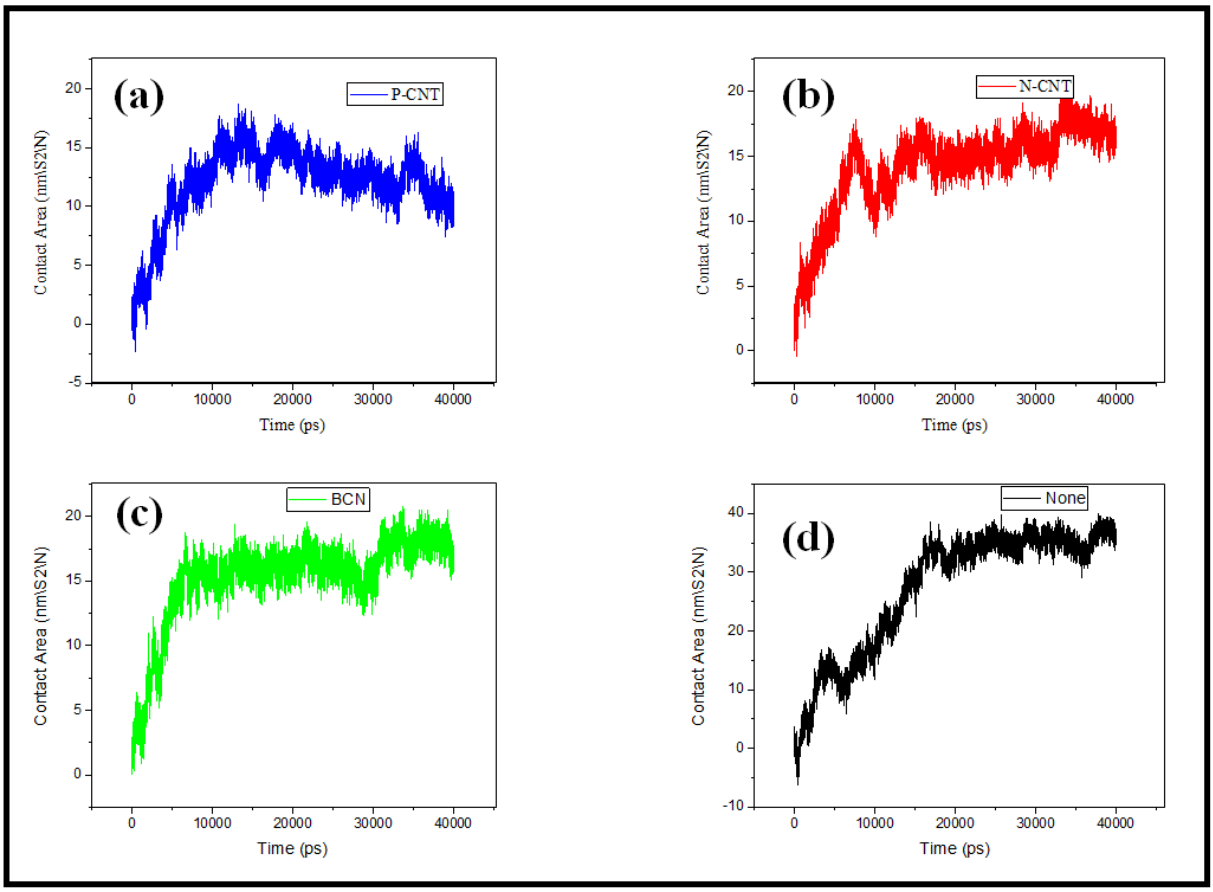

Figure 6 - Contact area of α-synuclein particles in the presence of a) P-CNT b) N-CNT c) BCN d) Without Nano Particle

The mean values of contact area variation in the presence of nanoparticles are less in the presence of nanoparticles (**Table 4**). The performance of all nanoparticles is positive in preventing the interaction of protein particles. However, BCN and P-CNT possess the highest and lowest average contact area variation and consequently effect on preventing the interaction of protein particles. Therefore, P-CNT is the most effective in preventing the interaction of α-synuclein protein particles and the most effective nanoparticle to prevent amyloid fibrillation.

Table 4 - Average contact area variation of α-synuclein particles in the presence/absence of nanoparticles

Nanoparticle	P-CNT	N-CNT	BCN	None
Contact Area (nm\S2\N)	11.99	14.18	15.23	27.24

4.4.Effect of α-synuclein and water hydrogen bonds connections on amyloid fibrillation process

Hydrogen bonding is the strongest intermolecular bond. The formation of an intermolecular bond between two molecules shows strong intermolecular interactions. Hydrogen bonds are formed between tiny hydrogen atoms and small electronegative atoms such as oxygen and nitrogen [51], [52]. The hydrogen bonds of α-synuclein water and protein reduce interactions between α-synuclein protein atoms. Lower interactions between α-synuclein atoms do not allow for alignment and aggregation in the relatively long α-synuclein chain. The higher the hydrogen bonds between water and α-synuclein proteins, the more difficult it is to form amyloid fibrils. The hydrogen interactions of water and the α-synuclein protein prevent the formation of amyloid fibrils. In this paper, to compare the ability of different nanoparticles to prevent the formation of amyloid fibrils, H_bond analysis between water and α-synuclein protein is taken. The H_bond analysis measures the hydrogen bonds created between water and α-synuclein protein. **Figure 7**shows diagrams of hydrogen bonds created between α-synuclein and water during the simulation, which decreases over time due to an increase in electrostatic interactions and VDW between nanoparticles and α-synuclein proteins. The slope of the reduction in hydrogen bonds is less in the simulation of α-synuclein protein in the presence of nanoparticles. The lower slope of the reduction in hydrogen bonds shows the effectiveness of nanoparticles in creating the right conditions for more hydrogen bonds in water and α-synuclein proteins. The diagrams from the H_bond analysis show the lowest slope of the decrease in hydrogen bonds in α-synuclein simulation in the presence of P-CNT over the simulation time. P-CNT nanoparticles have created the best conditions for hydrogen bonds between water and α-synuclein proteins.

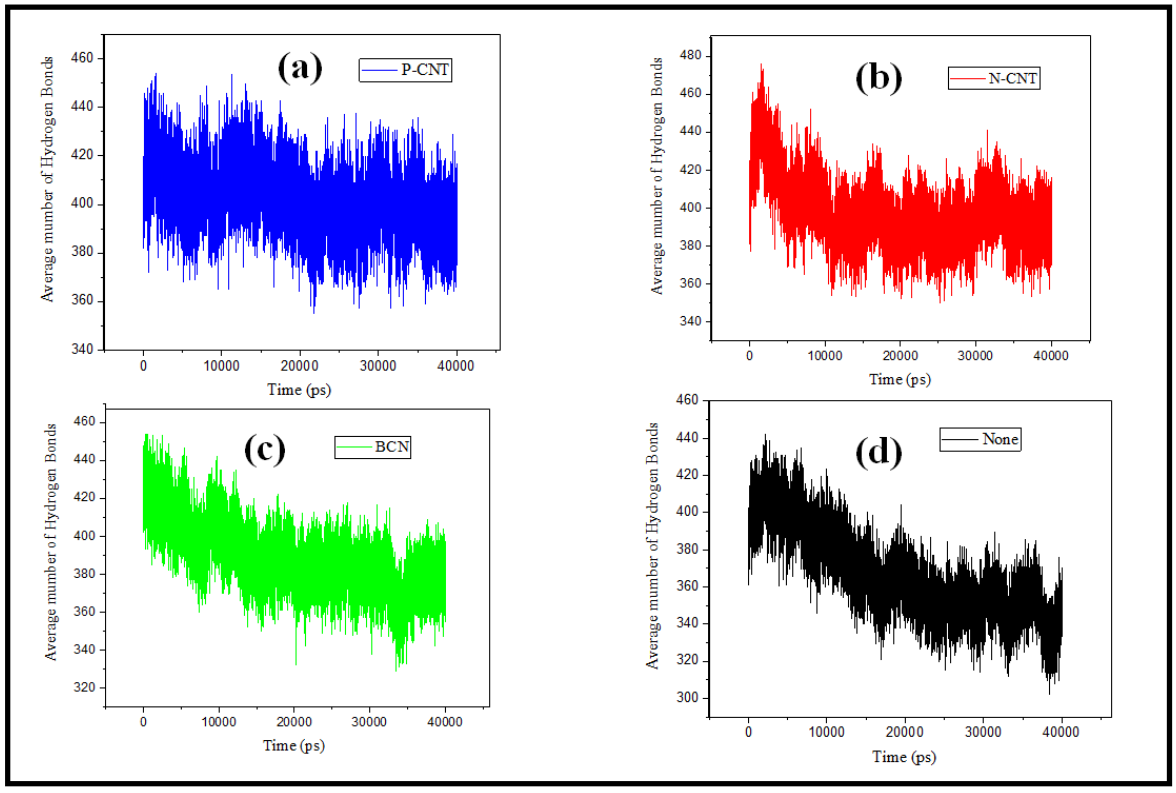

Figure 7 - Hydrogen bonds created between water and α-synuclein versus the simulation time for a) P-CNT b) N-CNT c) BCN d) Without Nano Particle

Table 5 shows the average hydrogen bonds created between water and α-synuclein in all simulations. The average hydrogen bonds between water and α-synuclein protein in the presence of nanoparticles are higher than the hydrogen bonds without nanoparticles. The greater the hydrogen bonds created, the more positive the effect of nanoparticles on the hydrogen bond between water and α-synuclein protein. Among the α-synuclein simulations in the presence of different nanoparticles, P-CNT and BCN had the highest and lowest mean hydrogen bonds, respectively. Although the use of BCN has provided better conditions for hydrogen bonding, it had the least effect compared to other nanoparticles. However, the effect of the P-CNT is more remarkable than other nanoparticles. More hydrogen bonds in the P-CNT simulation have further immersed α-synuclein in water, which leads to preventing foldings in the relatively long chain of α-synuclein. H_bond analysis shows that the P-CNT is the best compare to other nanoparticles to prevent amyloid fibrillation.

Table 5 - Average hydrogen bonds generated during simulation time in the presence of nanoparticles

Nanoparticle	P-CNT	N-CNT	BCN	None
Average Number of Hydrogen Bonds	402.34	397.49	389.05	366.92

4.5.α-synuclein particle density

Folding in the molecular structure causes the molecule particles to condense. The interactions of α-synuclein particles in the simulation bring the particles closer together and condense the protein. α-synuclein protein condensation provides the conditions for amyloid fibrillation. α-synuclein protein density during simulation is a good indicator for investigating the effect of nanoparticles on preventing amyloid fibrillation. Analyzing the Radius of Gyration, R_g, helps to investigate the α-synuclein protein density during the simulation. The higher the R_g, the higher the α-synuclein protein density. R_g calculates the distance of the molecule particles from the center of gravity of the molecule (Eq.6) [53]–[55]:

$$\mathrm{R_g} = \sqrt{\frac{\sum_{i=1}^{n} \mathrm{r_i^2 m_i}}{\sum_{i=1}^{n} \mathrm{m_i}}} \qquad (6)$$

where n is the number of particles, m_i, is the mass of the particle i, and r_i is the distance of the particle i from the center of gravity.

Figure 8 shows the α-synuclein R_g in the presence and absence of nanoparticles. R_g in all the simulations decrease after 15 nanoseconds. The density of the protein particles does not change much after 15 nanoseconds, and the amyloid protein structure has reached a relative equilibrium. The use of nanoparticles in the simulation system has increased R_g. Moreover, it reduced the density of the protein particles. P-CNT showed the highest R_g in the simulation compared to other cases.

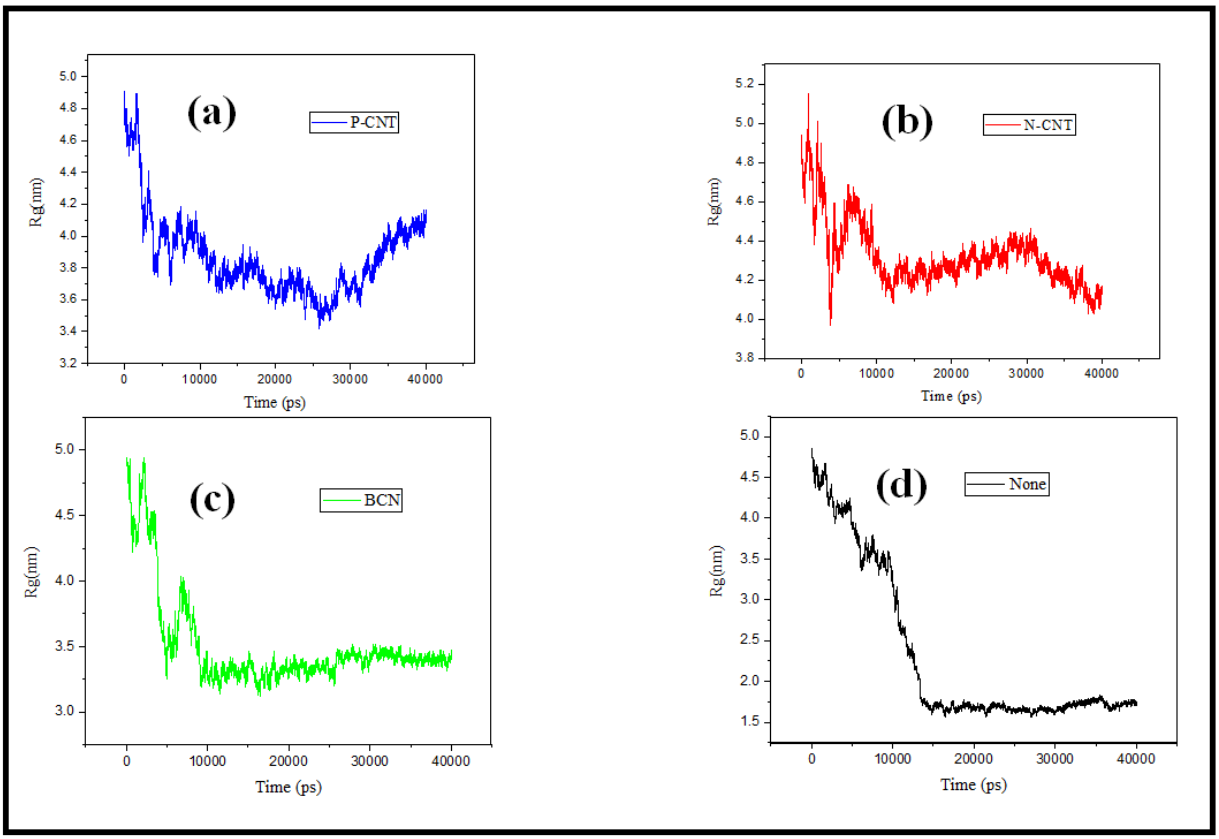

Figure 8 - Radius of Gyration of α-synuclein protein for a) P-CNT b) N-CNT c) BCN d) Without Nano Particle

To compare the ability of different nanoparticles to reduce the density of α-synuclein particles, the difference between the initial and final values of R_g was considered (**Table 6**). This difference decreased in the presence of nanoparticles, which indicates the positive effect of nanoparticles in preventing α-synuclein density. However, the highest and lowest difference occurs in the presence of BCN and P-CNT, respectively. Although BCN has reduced the density of amyloid particles, it has been less effective than other nanoparticles. This difference is negative in the presence of P-CNT, which means P-CNT has been the most effective nanoparticle to prevent the compaction of amyloid particles.

Table 6 - Differences between the initial and final R_g in the presence/absence of nanoparticles

Nanoparticle	P-CNT	N-CNT	BCN	None
Rg0-Rg40	0.77	0.79	1.48	3.07

4.6.α-synuclein protein stability

Folding in the α-synuclein protein chain provides better conditions for amyloid fibrillation. A-synuclein protein stability reduces the motility of its particles and creates the conditions for deformation in its chain. The use of different materials to create instability in the structure of the protein and thus further oscillations of its particles prevents amyloid fibrillation. In this paper, four nanoparticles are used to create instability in the α-synuclein protein structure. Root-Mean-Square Deviation (RMSD) and Root-Mean-Square Fluctuation (RMSF) analyzes have been used to compare the effect of nanoparticles used to create instability in the α-synuclein structure.

4.6.1.Stability assessment using RMSD analysis

Different particles oscillate to achieve their most stable state during simulation time. Fluctuations in simulation system particles are a perfect indicator for comparing the stability of different simulated systems. RMSD analysis is one of the most common analyzes in molecular dynamics simulation to investigate the oscillation of simulation system particles [56]–[59]. In RMSD analysis, the oscillation of the simulated system particles is calculated relative to a reference at different simulation times. RMSD values are calculated by Eq.7:

$$\mathrm{RMSD} = \sqrt{\frac{1}{\mathrm{n}}\sum_{\mathrm{i}=1}^{\mathrm{n}}(\mathrm{po_i(t)} - \mathrm{po}_r(\mathrm{t}))^2} \qquad (7)$$

where n shows the number of particles, $Po_i\ (t)$ shows the position of the particle i at time t, and $Po_r\ (t)$ shows the position of the reference particle at time t.

In creating instability in the α-synuclein protein structure, RMSD analysis for this protein has been taken in all simulations. The higher the oscillation of α-synuclein particles, the lower the stability of the protein structure.

Figure 9 shows the plot of RMSD in the presence and absence of nanoparticles versus simulation time. In all charts, we see a sudden jump in RMSD due to high particle oscillations in the system optimization phase. Particle fluctuations in all simulations decrease significantly after 15 nanoseconds compared to early simulations. The decreased fluctuations after 15 nanoseconds indicate relative stability in the simulation system. The slope of the RMSD diagram for protein simulation without nanoparticles after 15 nanoseconds is approximately zero. RMSD chart fluctuations in α-synuclein protein simulation in the presence of different nanoparticles have increased compared to the simulation of this protein without the use of nanoparticles. Increasing fluctuations in protein particles using nanoparticles have a positive effect on the use of nanoparticles in creating instability in the protein structure. However, the effect of P-CNT on the instability of the α-synuclein protein structure has been more significant than other nanoparticles.

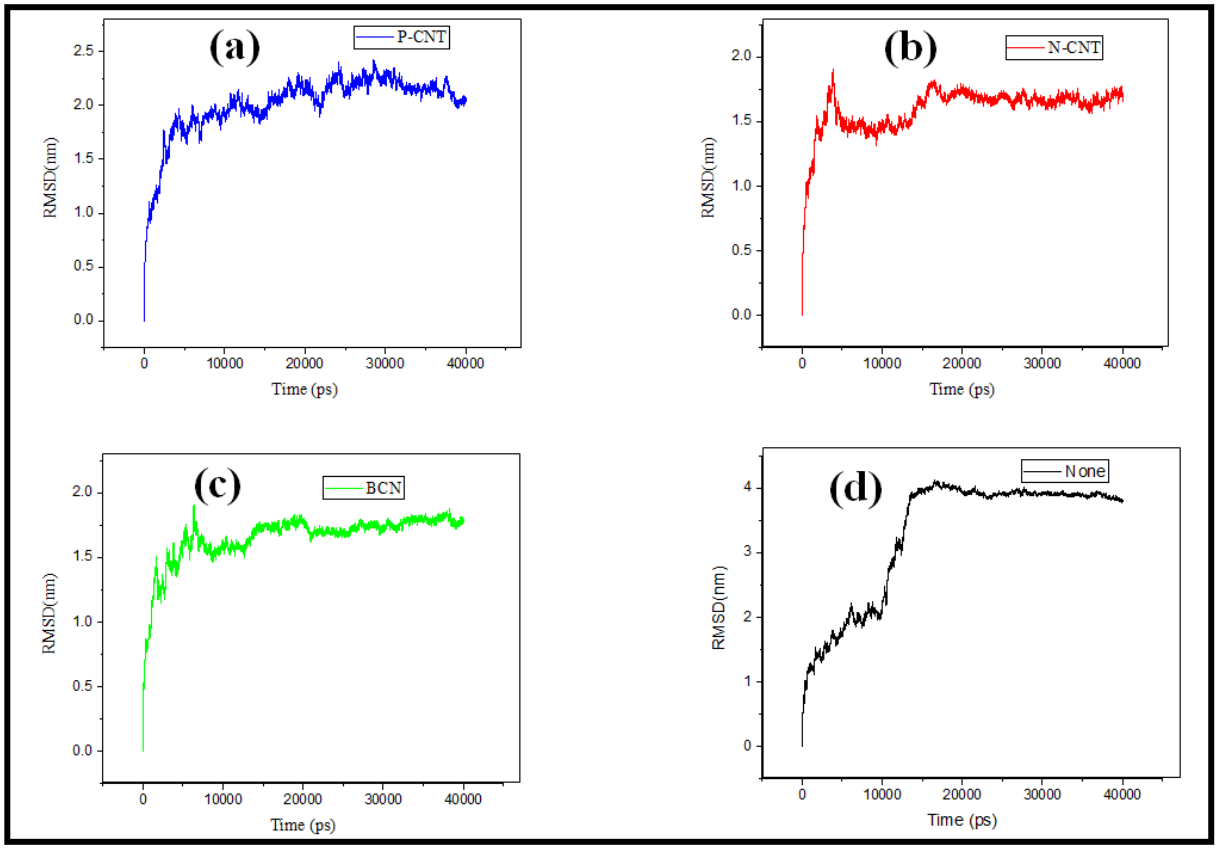

Figure 9 – α-synuclein protein RMSD for a) P-CNT b) N-CNT c) BCN d) Without Nano Particle

For a more accurate comparison of particle oscillations during simulation, RMSD values were derived using numerical derivative relationships. Then, the absolute geometric mean of the RMSD derivative was used to compare the particle fluctuations during the simulation. The higher the absolute value of the RMSD derivative, the greater the oscillation of the particles, and the greater the instability in the α-synuclein protein structure. **Table 7** shows the absolute geometric mean of the RMSD derivative calculated in the protein simulation in the presence of different nanoparticles. The mean RMSD derivative during α-synuclein protein simulation in the presence of nanoparticles was higher than the simulation of this protein without the presence of nanoparticles. The higher average RMSD derivative shows the positive effect of nanoparticles on the instability of the protein structure. Among nanoparticles, however, α-synuclein simulations in the presence of P-CNT and BCN had the highest and lowest RMSD derivative mining, respectively, during the simulation. Although the effect of BCN on creating instability in protein structure has been positive, it has created less instability in protein structure compared to other nanoparticles. Results showed that P-CNT is the best in creating instability in the α-synuclein protein structure and, consequently, the best nanoparticle to prevent amyloid fibrillation.

Table 7 - Absolute geometric mean of RMSD α-synuclein protein in nanoparticle simulations

Nanoparticle	P-CNT	N-CNT	BCN	None
Geometric Mean of RMSD Derivative *1000	3.87	3.61	3.53	3.45

4.6.2.Stability assessment using RMSF analysis

One of the appropriate analyzes to evaluate the oscillation rate of particles is using RMSF analysis. RMSF analysis makes it possible to calculate the fluctuations of all α-synuclein atoms to a single reference during the simulation. The greater the oscillation of α-synuclein atoms, the greater the instability of the α-synuclein protein molecular structure [60]–[63].

Figure 10 shows the RMSF analysis of all the simulations. This figure illustrates an increase in the fluctuations of protein atoms in the presence of nanoparticles. The use of nanoparticles has caused instability in the molecular structure of the α-synuclein protein. Different trends in RMSF sequences indicate different effects of nanoparticles on creating instability for various atoms.

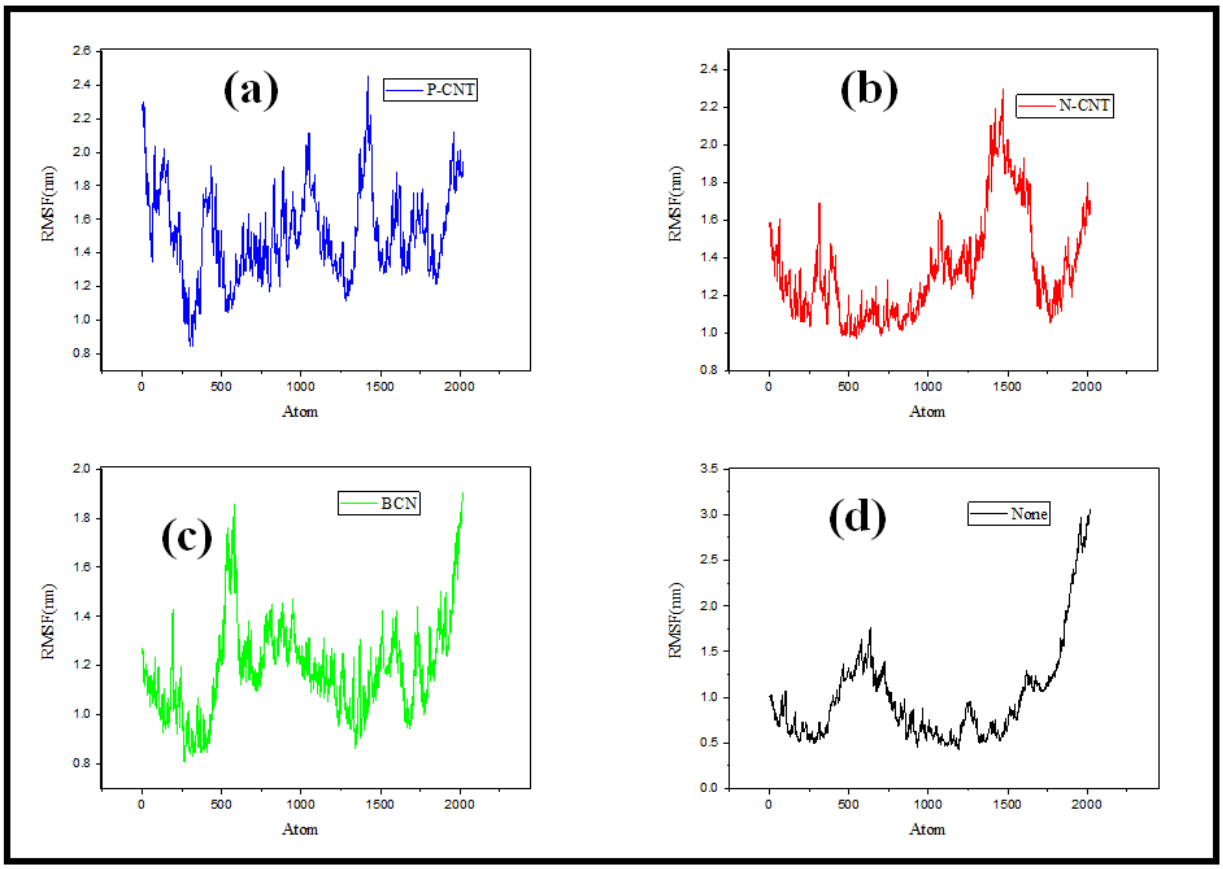

Figure 10 - α-synuclein protein RMSF for a) P-CNT b) N-CNT c) BCN d) Without Nano Particle

The calculated RMSF values for all atoms have been averaged to understand more details of the fluctuations of protein atoms (**Table 8**). The mean RMSF values in α-synuclein simulation in the presence of nanoparticles were higher compared to α-synuclein with no nanoparticles. Increasing RMSF values indicate a positive effect of nanoparticles on the instability of the α-synuclein molecule structure. α-synuclein simulations in the presence of P-CNT and BCN had the highest and lowest mean RMSF values during simulation, respectively. The effect of BCN has been positive in creating instability in the structure of α-synuclein, but less effective than other nanoparticles in creating instability in the molecular structure of α-synuclein. The most significant instability in the molecular structure of α-synuclein has been performed by P-CNT, which means that P-CNT is the best nanoparticle to prevent amyloid fibrillation.

Table 8 - Average RMSF for α-synuclein protein in the presence/absence of nanoparticles

Nanoparticle	P-CNT	N-CNT	BCN	None
Average of RMSF(nm)	1.51	1.34	1.19	1.01

5. Discussion

PD has no definite treatment; moreover, the drugs used for its treatment have high side effects; that's why this disease has been always in the center of the researchers' focus. Novel PD treatment technologies can help in the treatment of this disease. So far, various studies have addressed the effect of different materials including nanostructures on α-synuclein protein misfolding prevention which have shown promising results [32], [64]–[66]. The new generation of nanotubes that using from nitrogen and phosphorus dopants, has found significant applications [67]–[69]. Therefore, this study is aimed to investigate the effect of the doping nanotubes on the α-synuclein protein fibrillation. This generation of nanotubes has shown extraordinary ability to tune their properties. By doping at different concentrations, it is possible to engineer their features, in this study, new engineered structures of carbon nanotubes (CNTs) have been investigated for their use in the treatment of PD. Based on the results of this paper, the new generation of CNTs especially P-CNTs can prevent α-synuclein protein misfolding due to their higher interaction with α-synuclein protein. Energy analysis confirms proper interaction energy between all the doping CNTs and amyloids which can prevent amyloid misfolding. A comparison of the energy analysis with the secondary structure analysis also revealed that the higher the interaction energy between doping CNTs and α-synuclein, the higher the structural variations in the amyloid. The higher variation in the secondary structure also suggests the enhanced effectiveness of doping CNTs. Interaction energy and α-synuclein variations were higher in the case of P-CNT; thus it can be the best candidate for PD treatment. Gyration radius analysis also indicated a lower aggregation radius due to nanostructure interaction with α-synuclein in the case of P-CNT. A strong attractive force between the structures will lower the gyration radius. Therefore, the gyration radius analysis well indicated the better influence of P-CNT on the amyloids. Hydrogen bonds were also studied and the highest number of H-bonds

were also observed in P-CNT. Therefore, interaction energy due to hydrogen bonding was also higher in the case of P-CNT; similarly, Van der Waals and electrostatic energies were higher in this case. Other analyses such as interaction energy, secondary structure, gyration energy, and hydrogen bonding also confirmed that all the nanostructures, especially P-CNT, can be a proper choice for PD treatment. The simulation method was validated by comparison with the relevant references. RMSD and RMSF analyses also confirmed the simulation stability.

Comprehensive and valid molecular simulations of this paper well indicated the influence of the doping CNTs on the treatment of PD. These nanostructures prevent α-synuclein protein misfolding and eliminate the conditions required for aggregation of this protein particles; hence, Lewy body amyloids won't form. Therefore, this method can prevent the death of dopaminergic cells in the substantia nigra region and provide the dopamine required for extrapyramidal activities. Currently, the treatment methods of PD are based on alleviating the disease symptoms. The use of nanoparticles for preventing α-synuclein protein misfolding is a far more fundamental treatment method compared to the conventional methods. Moreover, due to the tubable structure of these nanoparticles, the problematic complications in the treatment of PD can be declined. This can suggest new applications for these nanoparticles in PD treatment and open new windows for future research works.

One of the simplest implications of nanoparticles could be their direct application in the treatment of PD. To this end, future studies should be able to use these nanoparticles in the pharmaceutical filed after their in-vitro tests and clinical trials. To accelerate this process, it is recommended to conduct targeted experimental studies to investigate the effect of the mentioned nanoparticles on preventing α-synuclein protein fibrillation. Different studies have suggested the suitability of carbon-based nanostructures (especially CNTs) as the drug nanocarrier [30], [70]–[72]. It seems that the application of these nanostructures (especially P-CNTs) to carry PD drugs can be an attractive topic for future studies. This can help in the simultaneous progress of classic and novel treatments for PD.

This study employed molecular dynamic simulations. The in-depth molecular insight, reduction of the cost and time required for studies in different fields has introduced molecular dynamic

simulations an incredible tool in the progression toward the objectives in various fields of science. Moreover, MD simulations make it possible to investigate the effect of nanoparticles under various conditions. This will result in more accurate and reliable findings. To use the MD-confirmed structures, they should be also confirmed by experimental studies, if the confirmed structures succeed in clinical tests, they can be employed in the prevention of PD. This study suggests a new way to use the new generation of nanotubes in the treatment of PD. This path should continue with laboratory, clinical and computational tests. In this case, we can hope that a great practical treatment for PD will be devloped.

6. Conclusion

Amyloid fibrillation caused by folding in α-synuclein protein causes PD. In this paper, the simulation of α-synuclein in the presence of four nanoparticles of carbon CNTs was considered to investigate the effect of nanoparticles in preventing α-synuclein chain distortion. Furthermore, energy, H_bond, R_g, RMSD, RMSF, secondary structure, and SASA analysis have been studied in this paper to scrutinize the effect of the presence of the nanoparticles. α-synuclein simulation in the presence of P-CNT had the highest energy value compared to other cases. Besides, energy analysis showed that P-CNT is the best nanoparticle to prevent α-synuclein chain folding. Hydrogen bonds between water and α-synuclein cause α-synuclein particles to disperse into the water and prevent the protein chain from becoming brittle. Most hydrogen bonds between α-synuclein and water occurred in the presence of P-CNT, N-CNT, and BCN. However, the P-CNT created the best conditions for hydrogen bonds between water and α-synuclein.

α-synuclein depletion is associated with an increase in helices and β_sheet structures and a decrease in Turn, Bend, and Bridge structures. Decreases in helices and β_sheet and increases in Turn, Bend, and Bridge in the secondary structure of α-synuclein occurred in the presence of P-CNT, N-CNT, and BCN, respectively. Analysis of the secondary structure showed that P-CNT is the best nanoparticle to prevent α-synuclein depletion. α-synuclein depletion causes the protein particles to condense. By analyzing R_g, the density of α-synuclein in the presence of nanoparticles was investigated. α-synuclein density was the lowest in simulation in the presence of P-CNT, N-CNT, and BCN, respectively. A higher contact area of α-synuclein during simulation indicates a further folding in this protein. α-synuclein particles have the lowest contact areas in simulation in the presence of P-CNT, N-CNT and BCN nanoparticles. The SASA analysis showed that, again, P-CNT is the best nanoparticle to prevent α-synuclein buildup. Last but not least, RMSF and RMSD analysis were performed to investigate the oscillation of α-synuclein particles. The derivative of RMSD values of α-synuclein particles and the mean oscillation of α-synuclein atoms had the highest values in simulation in the presence of P-CNT, N-CNT, and BCN nanoparticles, respectively. P-CNT's ability to cause instability in α-synuclein was more remarkable than other

cases. Overall, analyzes indicated that P-CNT is the best nanoparticle to prevent amyloid fibrillation. The results of this study recommend using P-CNT to prevent amyloid fibrillation.

7. Abbreviations

CNS:Central Nervous System

PD: Parkinson's Disease

MD: Molecular Dynamics

P-CNT: Phosphorus-doped Carbon NanoTube

N-CNT: Nitrogen-doped Carbon NanoTube

SPIONs :SuperParamagnetic Iron Oxide Nanoparticles

QDs :quantum dots ; CNTs: Carbon NanoTubes

BCN : nanotube co-duped with bromine and nitrogen

LINCS: Linear Constraint Solver

VDW :Van Der Walls

DSSP :Define Secondary Structure of Proteins

RMSD:Root-Mean-Square Deviation

RMSF:Root-Mean-Square Fluctuation

SASA:Solvent Accessible Surface Area

OPLS :Optimized Potentials for Liquid Simulations

8. Declarations

8.1. Ethics approval and consent to participate

Not applicable.

8.2. Availability of data and materials

All data generated or analyzed during this study are included in this published article.

8.3. Competing interests

The authors declare that they have no competing interests.

8.4. Funding

This research received no external funding.

8.5. Authors' contributions

Mohammad Khedri, Ahmad Miri Jahromi, Ehsan Alimohammadi, Reza Maleki, and Arash Nikzad conceived and designed the simulation; Mohammad Khedri and Ahmad Miri Jahromi carried out the simulations with, visualization of output data, analyze the data Milad Rezaian and Ahmad Miri Jahromi wrote the manuscript with support from Reza Maleki. interpretation of results was done by Nima Rezaei. The research was supervised and directed by Nima Rezaei. Authors contributed to investigation, conceptualization, methodology, analysis and writing-review & editing.

8.6. Acknowledgements

The authors wish to acknowledge Bahram Bastan for his support in Review & Editing. We would also like to show our appreciation to Mohammad Mahdi Nematollahi, Ali Mohammadi and Ebrahim ghasemy for sharing in editing of this work.

9. References

1. Stephenson J, Nutma E, van der Valk P, Amor S. Inflammation in CNS neurodegenerative diseases. Immunology. 2018;154(2):204–19.

2. Xicoy H, Wieringa B, Martens GJM. The SH-SY5Y cell line in Parkinson's disease research: a systematic review. Mol Neurodegener [Internet]. 2017;12(1):1–11. Available from: http://dx.doi.org/10.1186/s13024-017-0149-0

3. Limousin P, Foltynie T. Long-term outcomes of deep brain stimulation in Parkinson disease. Nat Rev Neurol [Internet]. 2019;15(4):234–42. Available from: http://dx.doi.org/10.1038/s41582-019-0145-9

4. Barker RA, Farrell K, Guzman NV, He X, Lazic SE, Moore S, et al. Designing stem-cell-based dopamine cell replacement trials for Parkinson's disease. Nat Med. 2019;25(July 2019).

5. Iwaki H, Tagawa M, Iwasaki K, Kawakami K, Nomoto M. Comparison of zonisamide with non-levodopa, anti-Parkinson's disease drugs in the incidence of Parkinson's disease-

relevant symptoms. J Neurol Sci [Internet]. 2019;402(December 2018):145–52. Available from: https://doi.org/10.1016/j.jns.2019.05.028

6. Cheong SL, Federico S, Spalluto G, Klotz KN, Pastorin G. The current status of pharmacotherapy for the treatment of Parkinson's disease: transition from single-target to multitarget therapy. Drug Discov Today [Internet]. 2019;24(9):1769–83. Available from: https://doi.org/10.1016/j.drudis.2019.05.003

7. Dawson TM, Golde TE, Lagier-Tourenne C. Animal models of neurodegenerative diseases. Nat Neurosci [Internet]. 2018;21(10):1370–9. Available from: http://dx.doi.org/10.1038/s41593-018-0236-8

8. Wu W hui, Sun X, Yu Y ping, Hu J, Zhao L, Liu Q, et al. TiO2 nanoparticles promote β-amyloid fibrillation in vitro. Biochem Biophys Res Commun. 2008;373(2):315–8.

9. Wang C, Telpoukhovskaia MA, Bahr BA, Chen X, Gan L. Endo-lysosomal dysfunction: a converging mechanism in neurodegenerative diseases. Curr Opin Neurobiol [Internet]. 2018;48(Figure 1):52–8. Available from: http://dx.doi.org/10.1016/j.conb.2017.09.005

10. Sheehan P, Yue Z. Deregulation of autophagy and vesicle trafficking in Parkinson's disease. Neurosci Lett [Internet]. 2019;697:59–65. Available from: https://doi.org/10.1016/j.neulet.2018.04.013

11. Yang, Pe[1] A. Mohebi et al., "Dissociable dopamine dynamics for learning and motivation," Nature, vol. 570, no. 7759, pp. 65–70, 2019 doi: 10. 1038/s4158.-019-1235-y. ngfe., Perlmutter JS, Benzinger TLS, Morris JC, Xu J. Dopamine D3 receptor: A neglected participant in Parkinson Disease pathogenesis and treatment? Ageing Res Rev [Internet]. 2020;57:100994. Available from: https://doi.org/10.1016/j.arr.2019.100994

12. Do J, McKinney C, Sharma P, Sidransky E. Glucocerebrosidase and its relevance to Parkinson disease. Mol Neurodegener. 2019;14(1):1–16.

13. Mohebi A, Pettibone JR, Hamid AA, Wong JMT, Vinson LT, Patriarchi T, et al. Dissociable dopamine dynamics for learning and motivation. Nature [Internet]. 2019;570(7759):65–

70. Available from: http://dx.doi.org/10.1038/s41586-019-1235-y

14. Surmeier DJ. Determinants of dopaminergic neuron loss in Parkinson's disease. FEBS J. 2018;285(19):3657–68.

15. Meissner WG, Frasier M, Gasser T, Goetz CG, Lozano A, Piccini P, et al. Priorities in Parkinson's disease research. Nat Rev Drug Discov [Internet]. 2011;10(5):377–93. Available from: http://dx.doi.org/10.1038/nrd3430

16. Meder D, Herz DM, Rowe JB, Lehéricy S, Siebner HR. The role of dopamine in the brain - lessons learned from Parkinson's disease. Neuroimage [Internet]. 2019;190:79–93. Available from: https://doi.org/10.1016/j.neuroimage.2018.11.021

17. Lee JY, Tuazon JP, Ehrhart J, Sanberg PR, Borlongan C V. Gutting the brain of inflammation: A key role of gut microbiome in human umbilical cord blood plasma therapy in Parkinson's disease model. J Cell Mol Med. 2019;23(8):5466–74.

18. Shao Y, Le W. Recent advances and perspectives of metabolomics-based investigations in Parkinson's disease. Mol Neurodegener. 2019;14(1):1–12.

19. Tremblay ME, Cookson MR, Civiero L. Glial phagocytic clearance in Parkinson's disease. Mol Neurodegener. 2019;14(1):1–14.

20. Donix M, Haussmann R, Helling F, Zweiniger A, Lange J, Werner A, et al. Cognitive impairment and medial temporal lobe structure in young adults with a depressive episode. J Affect Disord [Internet]. 2018;237(May):112–7. Available from: https://doi.org/10.1016/j.jad.2018.05.015

21. More SV, Choi DK. Promising cannabinoid-based therapies for Parkinson's disease: Motor symptoms to neuroprotection. Mol Neurodegener. 2015;10(1):1–26.

22. Sampaio TF, dos Santos EUD, de Lima GDC, dos Anjos RSG, da Silva RC, Asano AGC, et al. MAO-B and COMT Genetic Variations Associated With Levodopa Treatment Response in Patients With Parkinson's Disease. J Clin Pharmacol. 2018;58(7):920–6.

23. dos Santos EUD, Sampaio TF, Tenório dos Santos AD, Bezerra Leite FC, da Silva RC,

Crovella S, et al. The influence of SLC6A3 and DRD2 polymorphisms on levodopa-therapy in patients with sporadic Parkinson's disease. J Pharm Pharmacol. 2019;71(2):206–12.

24. Ge P, Dawson VL, Dawson TM. PINK1 and Parkin mitochondrial quality control: A source of regional vulnerability in Parkinson's disease. Mol Neurodegener. 2020;15(1):1–18.

25. Belli M, Ramazzotti M, Chiti F. Prediction of amyloid aggregation in vivo. EMBO Rep [Internet]. 2011;12(7):657–63. Available from: http://dx.doi.org/10.1038/embor.2011.116

26. Kumar A, Ganini D, Mason RP. Role of cytochrome c in α-synuclein radical formation: Implications of α-synuclein in neuronal death in Maneb- and paraquat-induced model of Parkinson's disease. Mol Neurodegener [Internet]. 2016;11(1):1–12. Available from: http://dx.doi.org/10.1186/s13024-016-0135-y

27. Hashimoto M, Rockenstein E, Mante M, Mallory M, Masliah E. β-synuclein inhibits α-synuclein aggregation: A possible role as an anti-Parkinsonian factor. Neuron. 2001;32(2):213–23.

28. Lassen, Michael;Gallus, Alexander;Raskob G. New England Journal NFL.pdf. N Engl J Med. 2010;363(26):2487–98.

29. Davenport A. Dialysis: A wearable dialysis device: The first step to continuous therapy. Nat Rev Nephrol [Internet]. 2016;12(9):512–4. Available from: http://dx.doi.org/10.1038/nrneph.2016.100

30. Raphey VR, Henna TK, Nivitha KP, Mufeedha P, Sabu C, Pramod K. Advanced biomedical applications of carbon nanotube. Mater Sci Eng C [Internet]. 2019;100(February):616–30. Available from: https://doi.org/10.1016/j.msec.2019.03.043

31. Iqbal Z, Aslam A, Ishaq M, Aamir M. Characteristic study of irregularity measures of some nanotubes. Can J Phys. 2019;97(10):1125–32.

32. Mohammad-Beigi H, Hosseini A, Adeli M, Ejtehadi MR, Christiansen G, Sahin C, et al. Mechanistic Understanding of the Interactions between Nano-Objects with Different

Surface Properties and α-Synuclein. ACS Nano. 2019;13(3):3243–56.

33. Frenkel D, Smit B, Tobochnik J, McKay SR, Christian W. Understanding Molecular Simulation. Comput Phys. 1997;11(4):351.

34. Huang J, Lemkul JA, Eastman PK, Mackerell AD. Molecular dynamics simulations using the drude polarizable force field on GPUs with OpenMM: Implementation, validation, and benchmarks. J Comput Chem. 2018;1–8.

35. Rezaian M, Maleki R, Dahroud MD, Alamdari A, Alimohammadi M. pH-sensitive co-adsorption/release of doxorubicin and paclitaxel by carbon nanotube, fullerene, and graphene oxide in combination with N-isopropylacrylamide: A molecular dynamics study. Biomolecules. 2018;8(4):1–21.

36. Mortazavifar A, Raissi H, Akbari A. DFT and MD investigations on the functionalized boron nitride nanotube as an effective drug delivery carrier for Carmustine anticancer drug. J Mol Liq [Internet]. 2019;276:577–87. Available from: https://doi.org/10.1016/j.molliq.2018.12.028

37. Ulmer TS, Bax A, Cole NB, Nussbaum RL. Structure and dynamics of micelle-bound human α-synuclein. J Biol Chem. 2005;280(10):9595–603.

38. Wang L, Xu J, Wang X, Cheng Z, Xu J. Facile preparation of N-rich functional polymer with porous framework as QCM sensing material for rapid humidity detection. Sensors Actuators, B Chem [Internet]. 2019;288(February):289–97. Available from: https://doi.org/10.1016/j.snb.2019.02.058

39. Robertson MJ, Qian Y, Robinson MC, Tirado-Rives J, Jorgensen WL. Development and Testing of the OPLS-AA/M Force Field for RNA. J Chem Theory Comput. 2019;15(4):2734–42.

40. Itliong JN, Villagracia ARC, Moreno JL V., Rojas KIM, Bernardo GPO, David MY, et al. Investigation of reverse ionic diffusion in forward-osmosis-aided dewatering of microalgae: A molecular dynamics study. Bioresour Technol [Internet].

2019;279(January):181–8. Available from: https://doi.org/10.1016/j.biortech.2019.01.109

41. Martoňák R, Donadio D, Oganov AR, Parrinello M. Crystal structure transformations in SiO2 from classical and ab initio metadynamics. Nat Mater. 2006;5(8):623–6.

42. Damghani T, Sedghamiz T, Sharifi S, Pirhadi S. Critical c-Met-inhibitor interactions resolved from molecular dynamics simulations of different c-Met complexes. J Mol Struct [Internet]. 2020;1203:127456. Available from: https://doi.org/10.1016/j.molstruc.2019.127456

43. Dehury B, Behera SK, Mahapatra N. Structural dynamics of Casein Kinase I (CKI) from malarial parasite Plasmodium falciparum (Isolate 3D7): Insights from theoretical modelling and molecular simulations. J Mol Graph Model [Internet]. 2017;71:154–66. Available from: http://dx.doi.org/10.1016/j.jmgm.2016.11.012

44. Maleki R, Afrouzi HH, Hosseini M, Toghraie D, Piranfar A, Rostami S. pH-sensitive loading/releasing of doxorubicin using single-walled carbon nanotube and multi-walled carbon nanotube: A molecular dynamics study. Comput Methods Programs Biomed [Internet]. 2020;186:105210. Available from: https://doi.org/10.1016/j.cmpb.2019.105210

45. Miceli M, Muscat S, Morbiducci U, Cavaglià M, Deriu MA. Ultrasonic waves effect on S-shaped β-amyloids conformational dynamics by non-equilibrium molecular dynamics. J Mol Graph Model [Internet]. 2020;96:107518. Available from: https://doi.org/10.1016/j.jmgm.2019.107518

46. Turner M, Mutter ST, Kennedy-Britten OD, Platts JA. Molecular dynamics simulation of aluminium binding to amyloid-β and its effect on peptide structure. PLoS One. 2019;14(6):1–14.

47. Turner M, Mutter ST, Kennedy-Britten OD, Platts JA. Replica exchange molecular dynamics simulation of the coordination of Pt(ii)-Phenanthroline to amyloid-β. RSC Adv. 2019;9(60):35089–97.

48. Murray IVJ, Giasson BI, Quinn SM, Koppaka V, Axelsen PH, Ischiropoulos H, et al. Role of α-synuclein carboxy-terminus on fibril formation in vitro. Biochemistry. 2003;42(28):8530–40.

49. Pereira GRC, Da Silva ANR, Do Nascimento SS, De Mesquita JF. In silico analysis and molecular dynamics simulation of human superoxide dismutase 3 (SOD3) genetic variants. J Cell Biochem. 2019;120(3):3583–98.

50. Arifuzzaman M, Mitra S, Das R, Hamza A, Absar N, Dash R. In silico analysis of nonsynonymous single-nucleotide polymorphisms (nsSNPs) of the SMPX gene. Ann Hum Genet. 2020;84(1):54–71.

51. Fang H, Tang Z, Liu X, Huang Y, Sun CQ. Discriminative ionic capabilities on hydrogen-bond transition from the mode of ordinary water to (Mg, Ca, Sr)(Cl, Br) 2 hydration. J Mol Liq [Internet]. 2019;279:485–91. Available from: https://doi.org/10.1016/j.molliq.2019.01.147

52. Zhong Y, Chen Y, Feng X, Sun Y, Cui S, Li X, et al. Hydrogen-bond facilitated intramolecular proton transfer in excited state and fluorescence quenching mechanism of flavonoid compounds in aqueous solution. J Mol Liq [Internet]. 2020;302:112562. Available from: https://doi.org/10.1016/j.molliq.2020.112562

53. Kharazian B, Lohse SE, Ghasemi F, Raoufi M, Saei AA, Hashemi F, et al. Bare surface of gold nanoparticle induces inflammation through unfolding of plasma fibrinogen. Sci Rep [Internet]. 2018;8(1):1–9. Available from: http://dx.doi.org/10.1038/s41598-018-30915-7

54. Maleki R, Afrouzi HH, Hosseini M, Toghraie D, Rostami S. Molecular dynamics simulation of Doxorubicin loading with N-isopropyl acrylamide carbon nanotube in a drug delivery system. Comput Methods Programs Biomed [Internet]. 2020;184:105303. Available from: https://doi.org/10.1016/j.cmpb.2019.105303

55. Ajori S, Ansari R, Haghighi S. A molecular dynamics study on the buckling behavior of cross-linked functionalized carbon nanotubes under physical adsorption of polymer chains. Appl Surf Sci [Internet]. 2018;427:704–14. Available from:

https://doi.org/10.1016/j.apsusc.2017.08.049

56. Saini RK, Thakur H, Goyal B. Effect of Piedmont mutation (L34V) on the structure, dynamics, and aggregation of Alzheimer's Aβ40 peptide. J Mol Graph Model [Internet]. 2020;97:107571. Available from: https://doi.org/10.1016/j.jmgm.2020.107571

57. Bertaccini EJ, Tradelia JR, Lindane E. Normal-mode analysis of the glycine alpha1 receptor by three separate methods. J Chem Inf Model. 2007;47(4):1572–9.

58. Rahmatabadi SS, Sadeghian I, Ghasemi Y, Sakhteman A, Hemmati S. Identification and characterization of a sterically robust phenylalanine ammonia-lyase among 481 natural isoforms through association of in silico and in vitro studies. Enzyme Microb Technol [Internet]. 2019;122(June 2018):36–54. Available from: https://doi.org/10.1016/j.enzmictec.2018.12.006

59. Farhadian S, Shareghi B, Asgharzadeh S, Rajabi M, Asadi H. Structural characterization of α-chymotrypsin after binding to curcumin: Spectroscopic and computational analysis of their binding mechanism. J Mol Liq [Internet]. 2019;289:111111. Available from: https://doi.org/10.1016/j.molliq.2019.111111

60. Chairatana P, Niramitranon J, Pongprayoon P. Dynamics of human defensin 5 (HD5) self-assembly in solution: Molecular simulations/insights. Comput Biol Chem [Internet]. 2019;83(April 2018):107091. Available from: https://doi.org/10.1016/j.compbiolchem.2019.107091

61. Liu J, Wei B, Che C, Gong Z, Jiang Y, Si M, et al. Enhanced stability of manganese superoxide dismutase by amino acid replacement designed via molecular dynamics simulation. Int J Biol Macromol [Internet]. 2019;128:297–303. Available from: https://doi.org/10.1016/j.ijbiomac.2019.01.126

62. Zaboli M, Raissi H, Zaboli M, Farzad F, Torkzadeh-Mahani M. Stabilization of D-lactate dehydrogenase diagnostic enzyme via immobilization on pristine and carboxyl-functionalized carbon nanotubes, a combined experimental and molecular dynamics simulation study. Arch Biochem Biophys [Internet]. 2019;661(November 2018):178–86.

Available from: https://doi.org/10.1016/j.abb.2018.11.019

63. Rezapour N, Rasekh B, Mofradnia SR, Yazdian F, Rashedi H, Tavakoli Z. Molecular dynamics studies of polysaccharide carrier based on starch in dental cavities. Int J Biol Macromol [Internet]. 2019;121:616–24. Available from: https://doi.org/10.1016/j.ijbiomac.2018.10.027

64. Mohammadi S, Nikkhah M. Carbon Nanotubes as Potential Agents against Fibrillation of α-Synuclein , a Parkinson ' s Disease-Related Protein. 2019;4(2):127–33.

65. Javdani N, Rahpeyma SS, Ghasemi Y, Raheb J. Effect of superparamagnetic nanoparticles coated with various electric charges on α-synuclein and β-amyloid proteins fibrillation process. Int J Nanomedicine. 2019;14:799–808.

66. Palazzi L, Bruzzone E, Bisello G, Leri M, Stefani M, Bucciantini M, et al. Oleuropein aglycone stabilizes the monomeric α-synuclein and favours the growth of non-toxic aggregates. Sci Rep. 2018;8(1):1–17.

67. Blackburn JL, Ferguson AJ, Cho C, Grunlan JC. Carbon-Nanotube-Based Thermoelectric Materials and Devices. Adv Mater. 2018;30(11):1–35.

68. Schroeder V, Savagatrup S, He M, Lin S, Swager TM. Carbon nanotube chemical sensors. Chem Rev. 2019;119(1):599–663.

69. Yang Z, Tian J, Yin Z, Cui C, Qian W, Wei F. Carbon nanotube- and graphene-based nanomaterials and applications in high-voltage supercapacitor: A review. Carbon N Y [Internet]. 2019;141:467–80. Available from: https://doi.org/10.1016/j.carbon.2018.10.010

70. Vashist A, Kaushik A, Vashist A, Sagar V, Ghosal A, Gupta YK, et al. Advances in Carbon Nanotubes–Hydrogel Hybrids in Nanomedicine for Therapeutics. Adv Healthc Mater. 2018;7(9):1–21.

71. Saliev T. The Advances in Biomedical Applications of Carbon Nanotubes. C. 2019;5(2):29.

72. Mahajan S, Patharkar A, Kuche K, Maheshwari R, Deb PK, Kalia K, et al. Functionalized

carbon nanotubes as emerging delivery system for the treatment of cancer. Int J Pharm [Internet]. 2018;548(1):540–58. Available from: https://doi.org/10.1016/j.ijpharm.2018.07.027

Figures

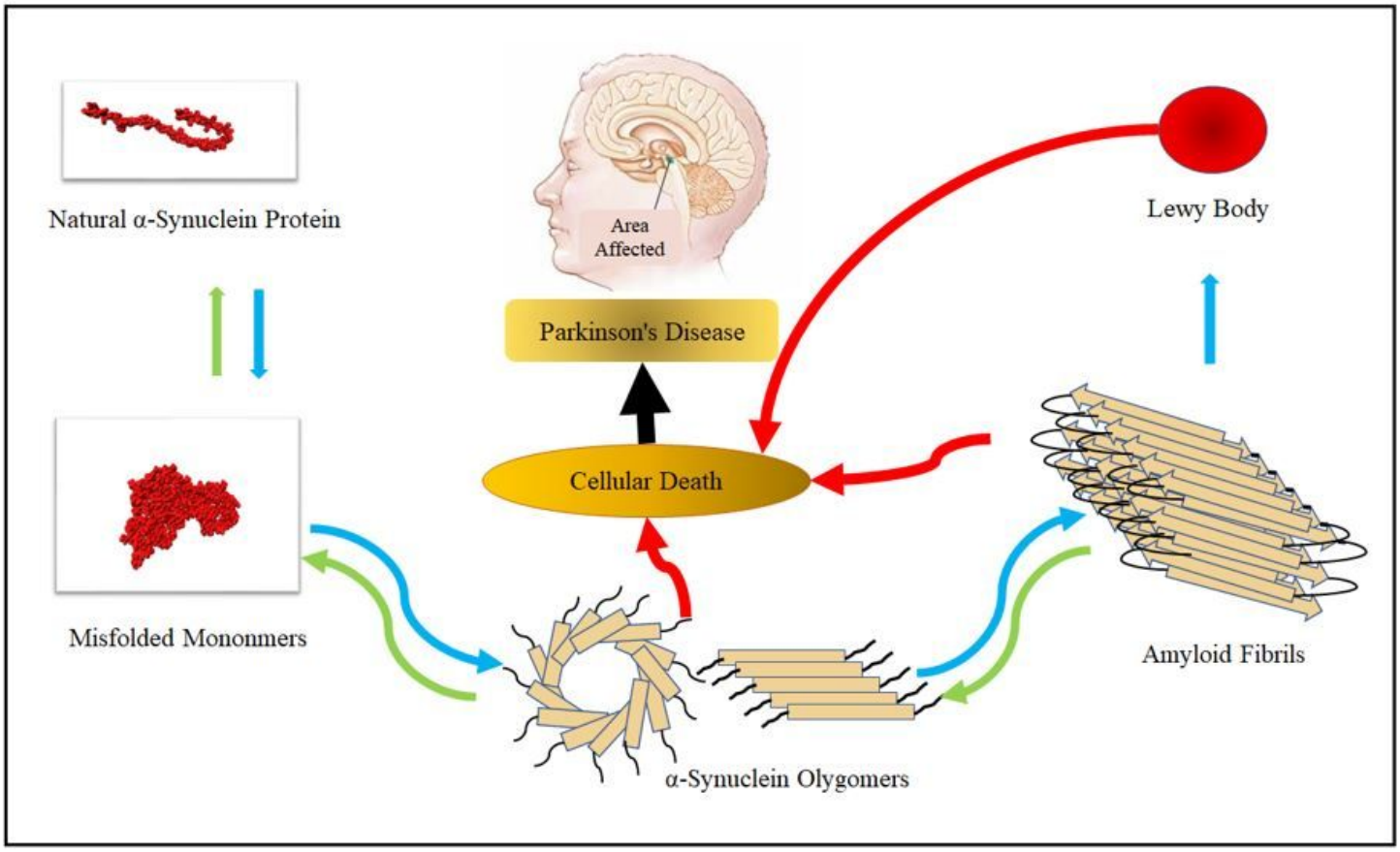

Figure 1

Amyloid fibrillation process and its role in the formation of PD

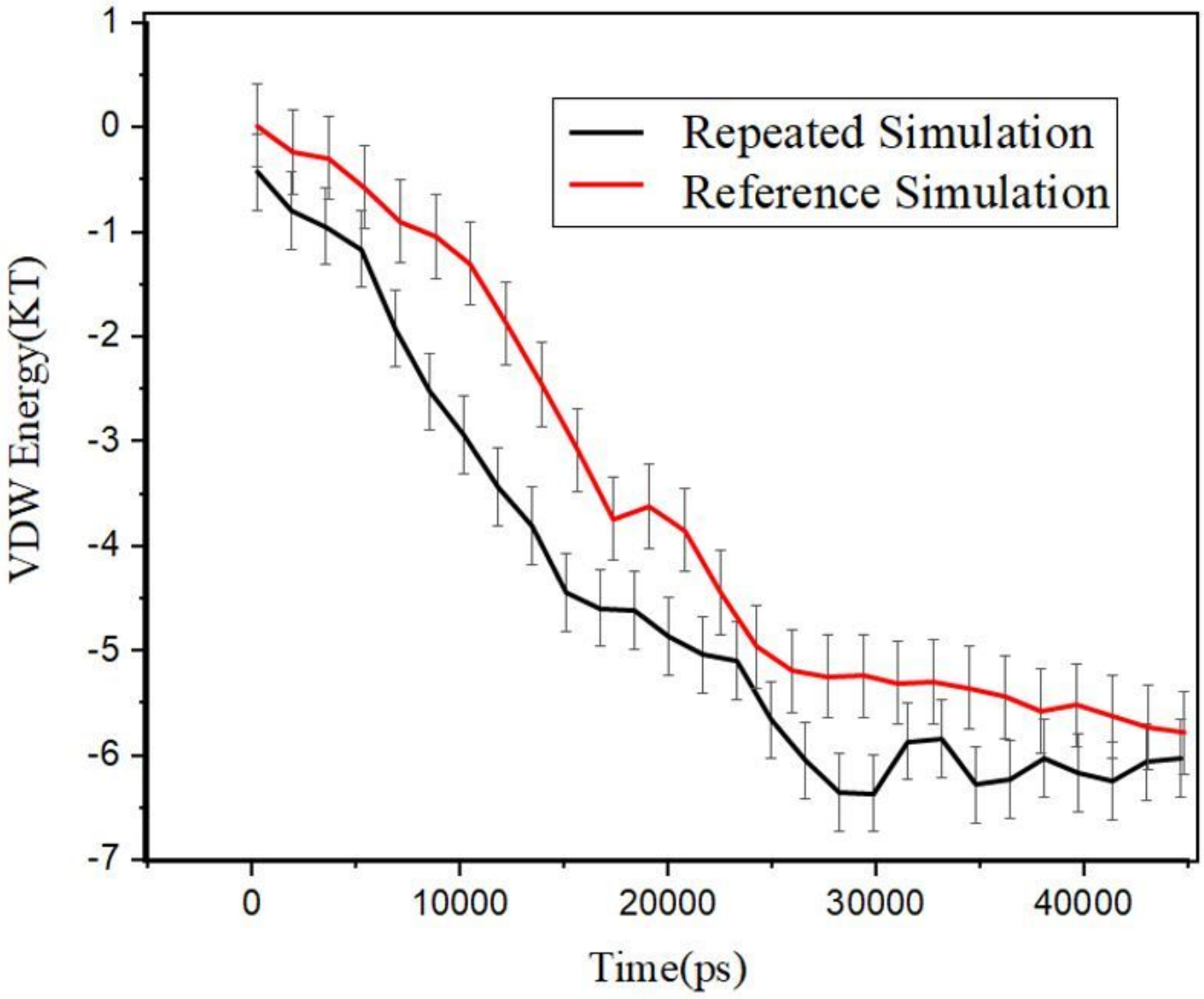

Figure 2

VDW energy in this study and [32] to validate the results

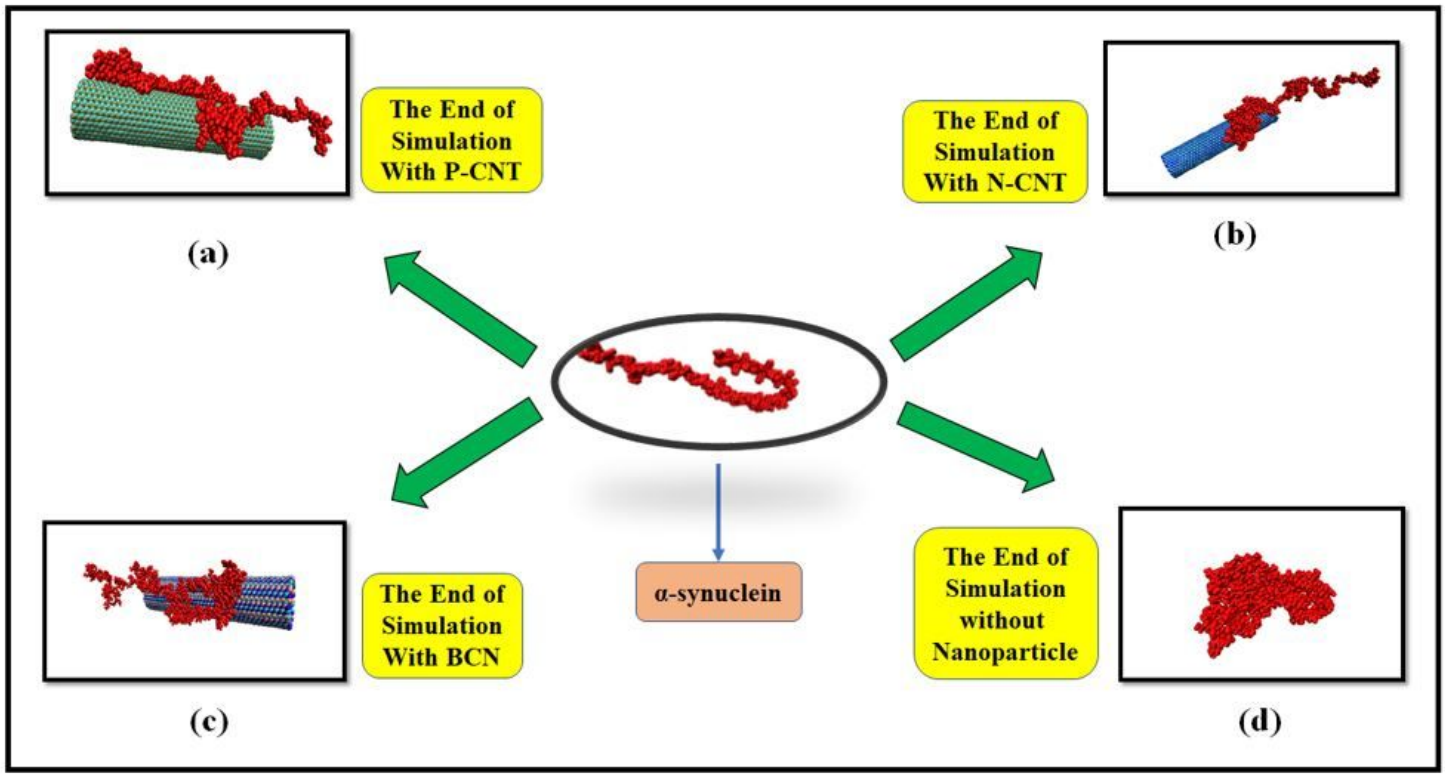

Figure 3

Results of α-synuclein simulation after 40 nanoseconds with a) P-CNT b) N-CNT c) BCN d) Without Nano Particle

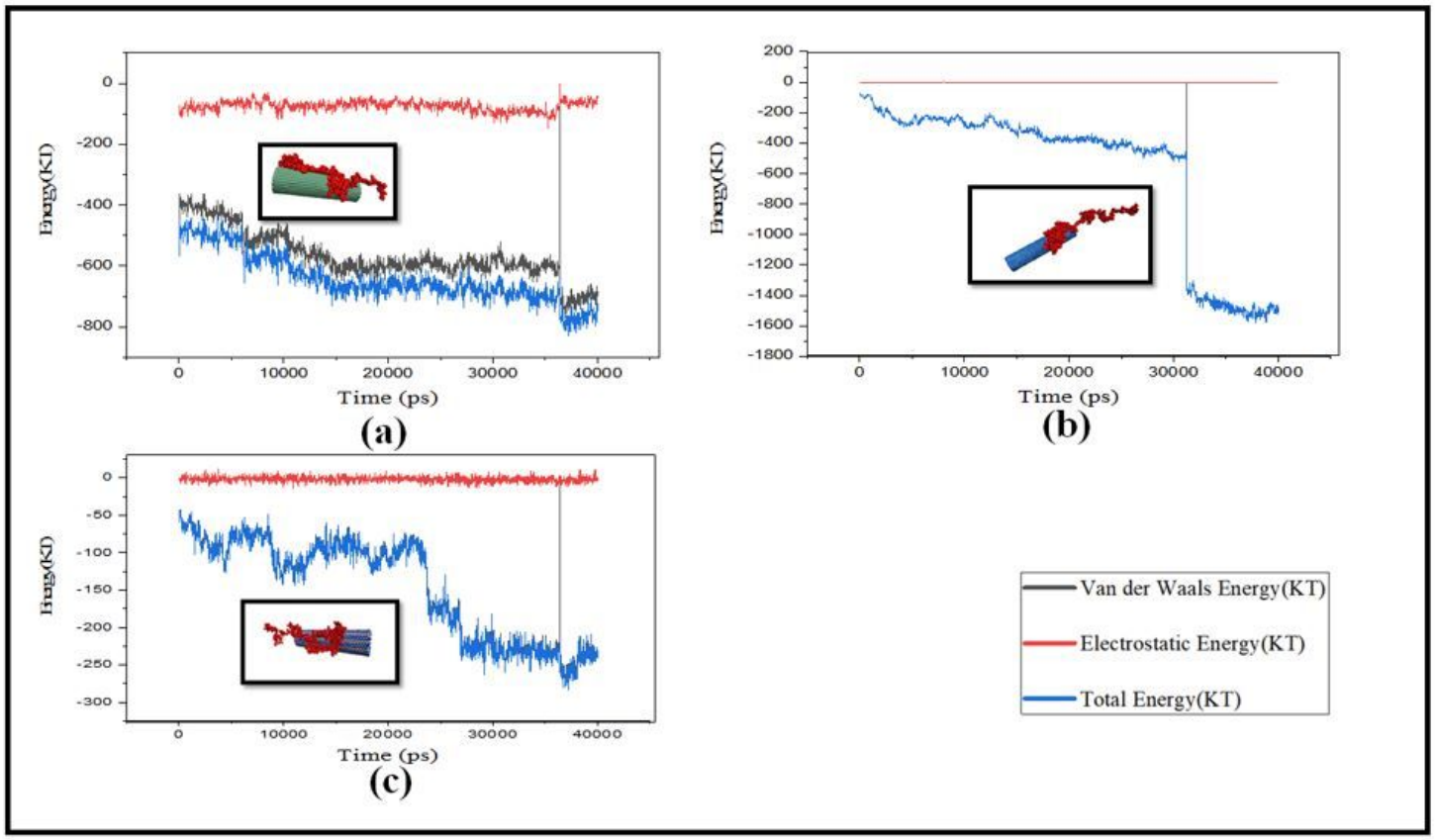

Figure 4

Nanoparticle simulation energy diagrams a) P-CNT b)N-CNT c) BCN and α-synuclein in protein over 40 nanoseconds

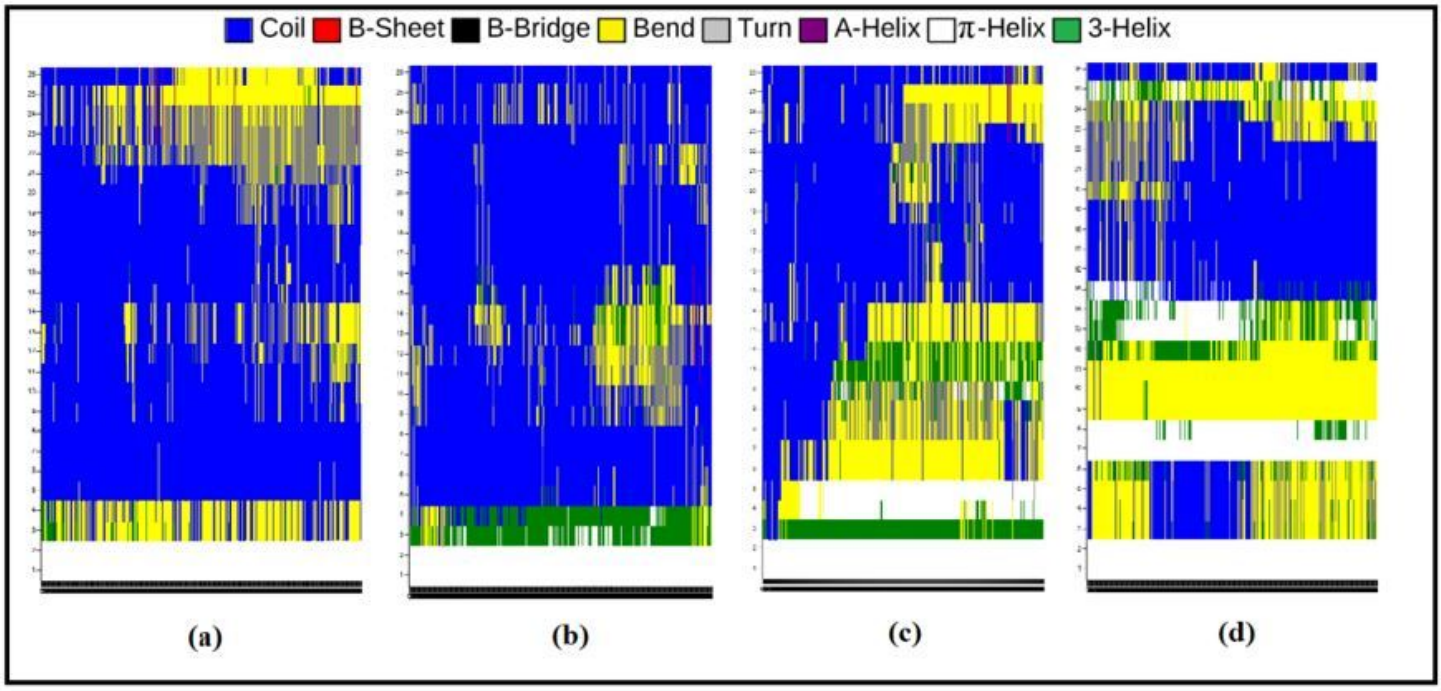

Figure 5

the secondary structure of α-synuclein in the presence of a) P-CNT b) N-CNT c) BCN d) Without Nano Particle

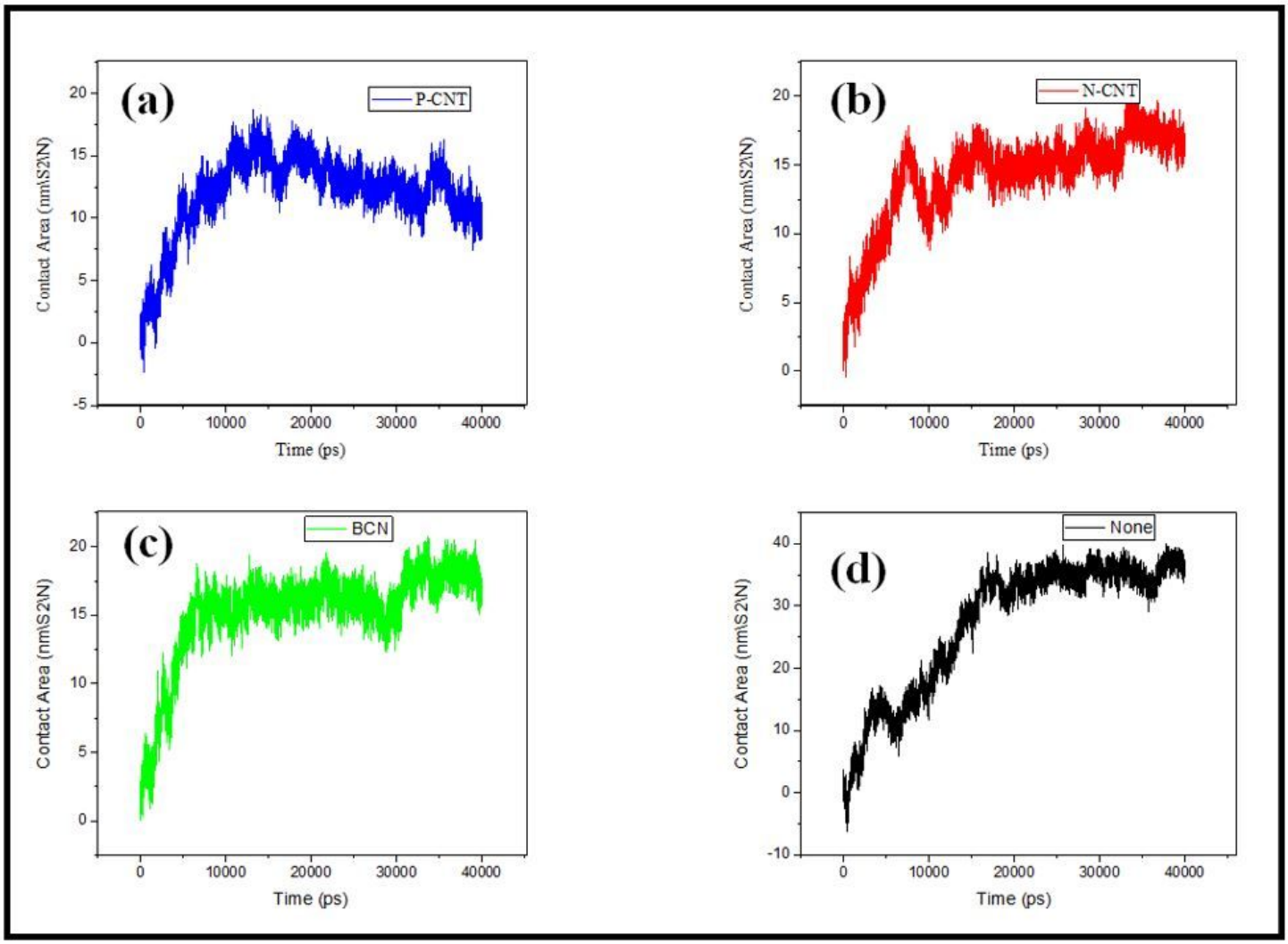

Figure 6

Contact area of α-synuclein particles in the presence of a) P-CNT b) N-CNT c) BCN d) Without Nano Particle

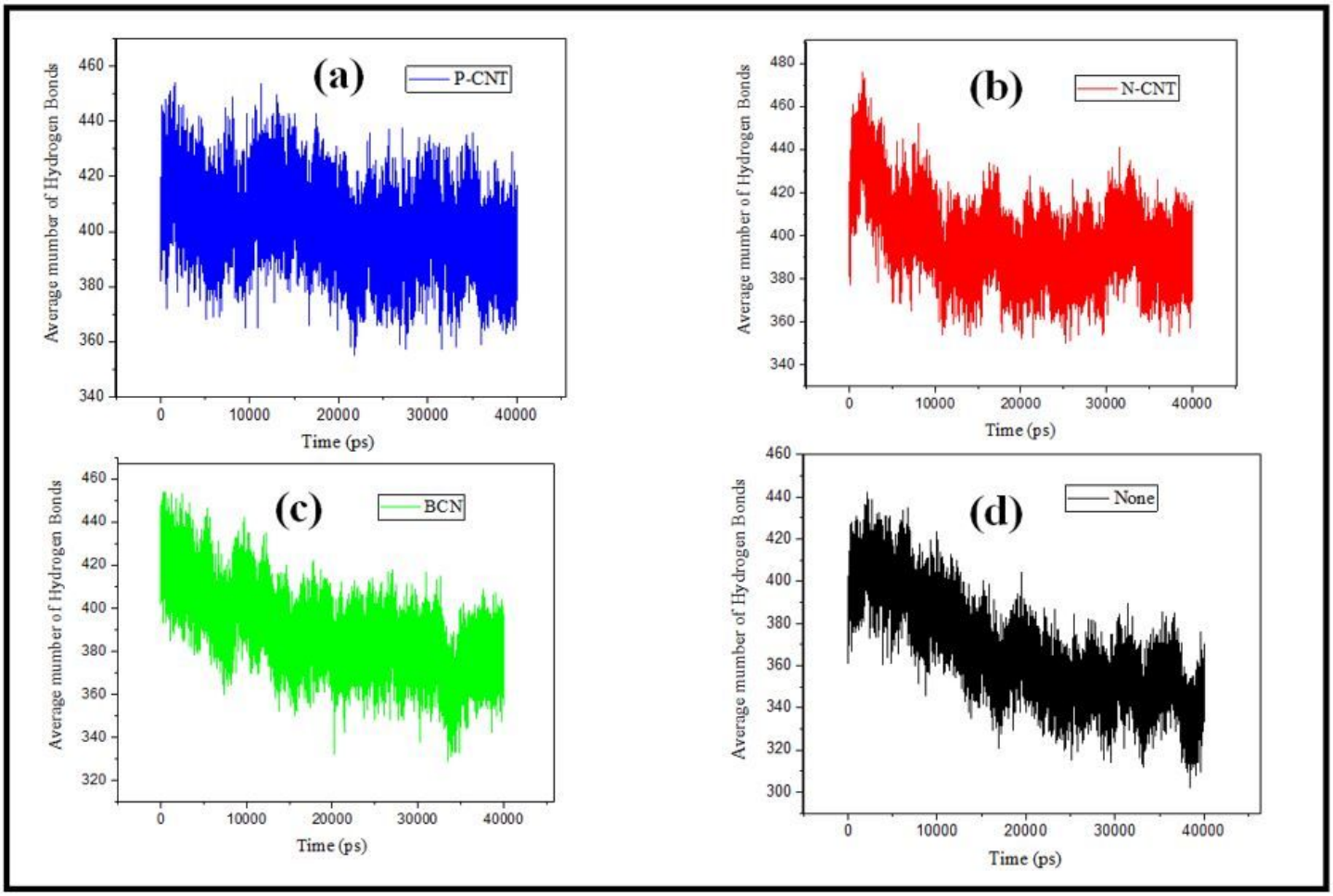

Figure 7

Hydrogen bonds created between water and α-synuclein versus the simulation time for a) P-CNT b) N-CNT c) BCN d) Without Nano Particle

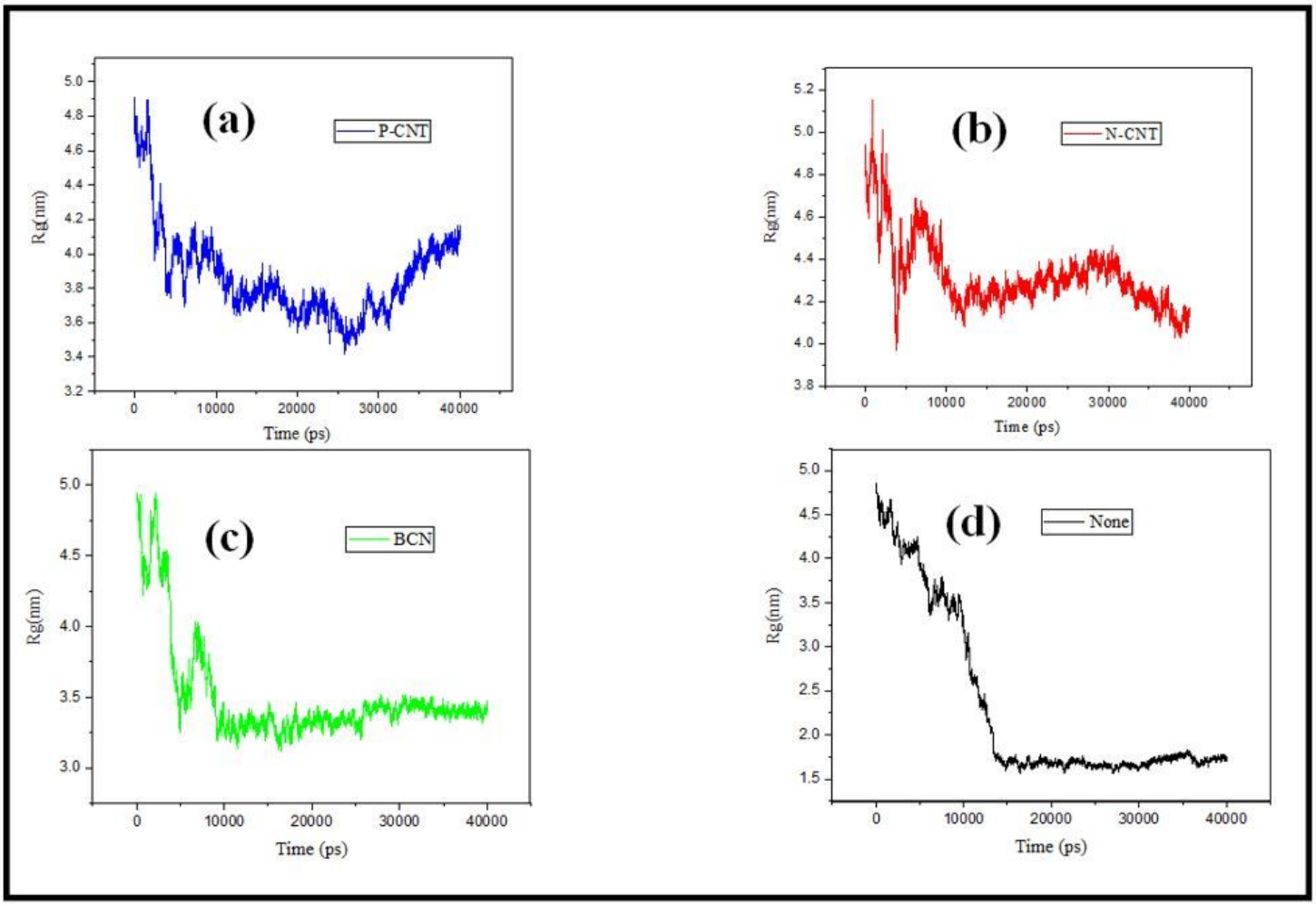

Figure 8

Radius of Gyration of α-synuclein protein for a) P-CNT b) N-CNT c) BCN d) Without Nano Particle

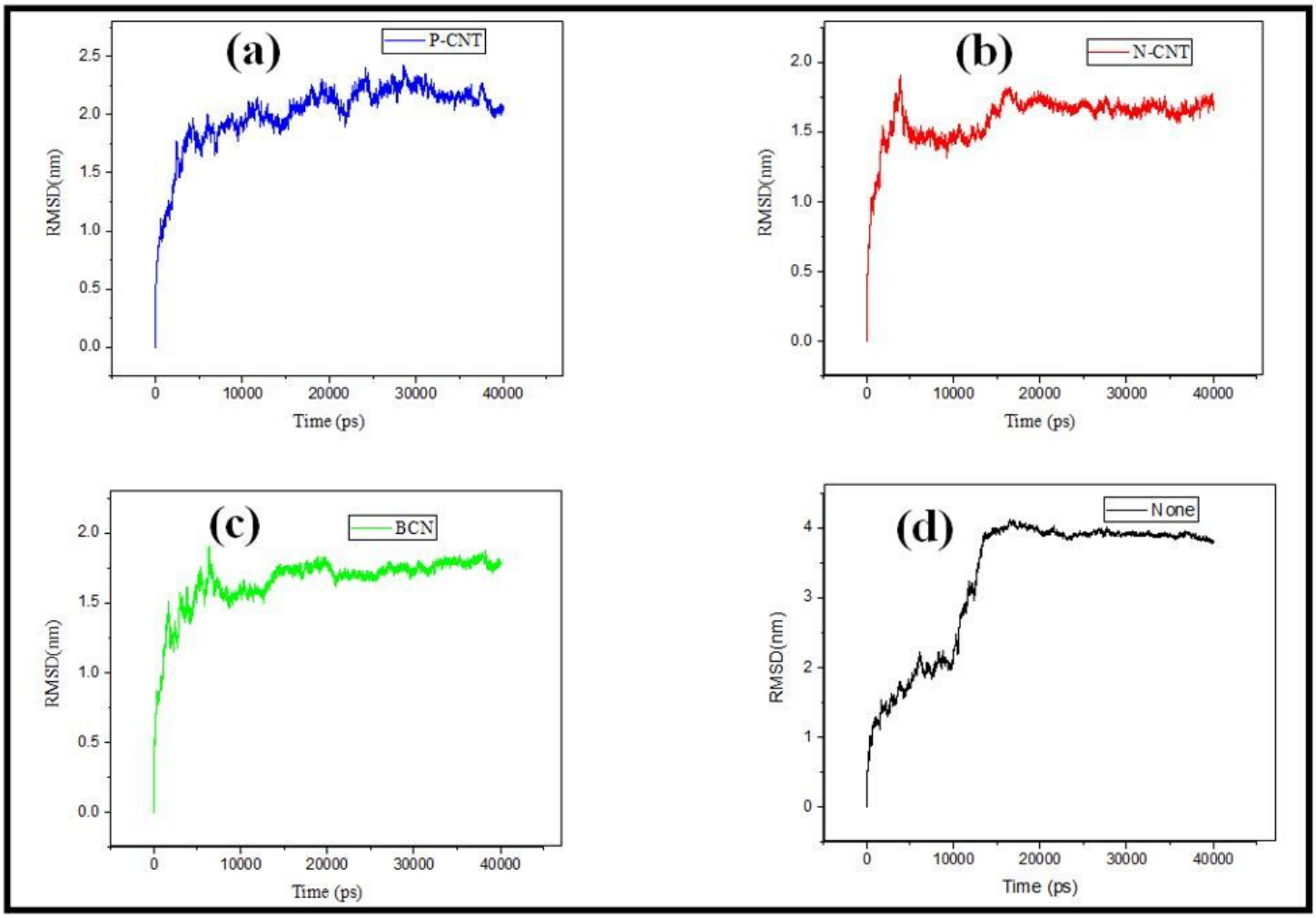

Figure 9

α-synuclein protein RMSD for a) P-CNT b) N-CNT c) BCN d) Without Nano Particle

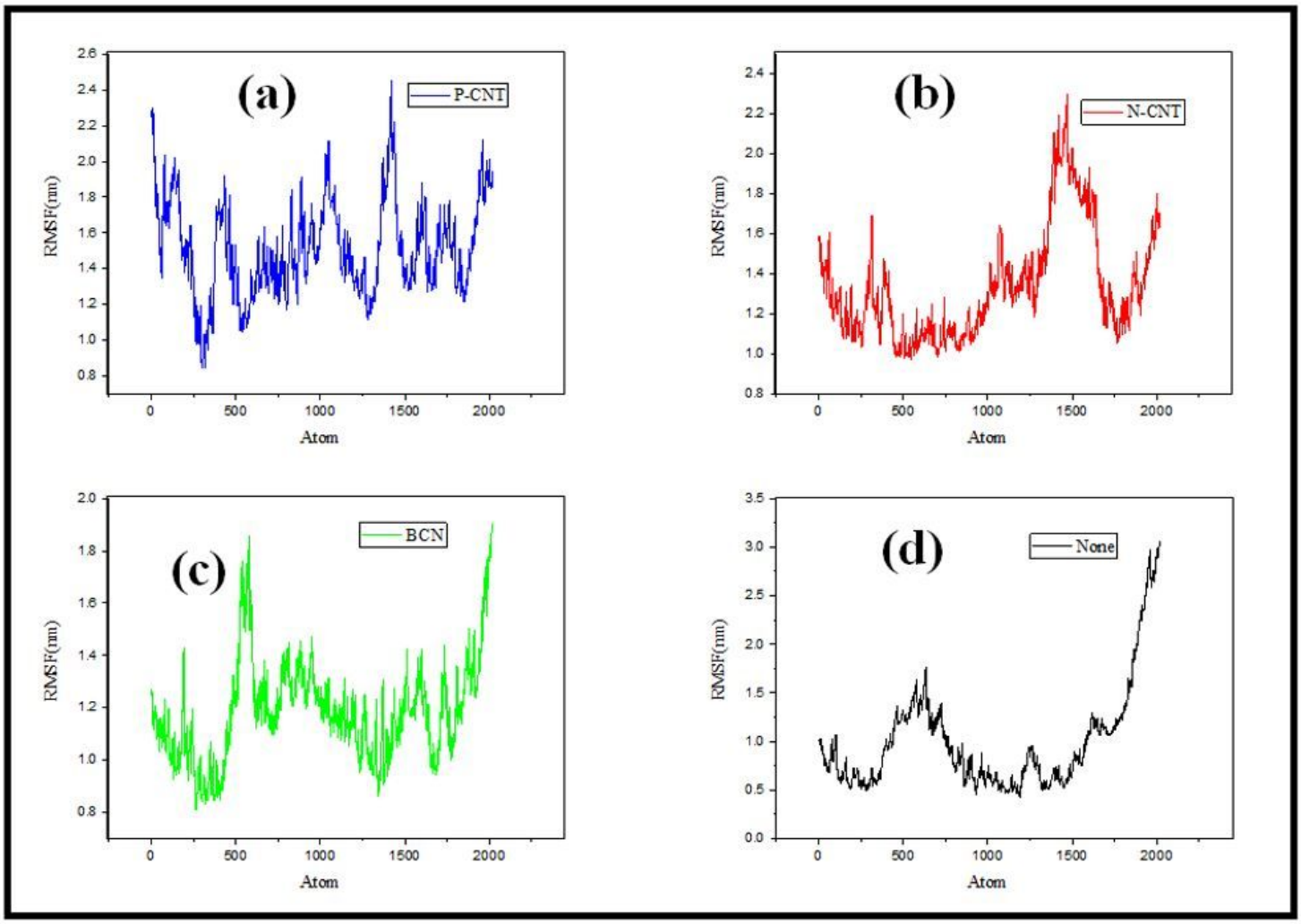

Figure 10

α-synuclein protein RMSF for a) P-CNT b) N-CNT c) BCN d) Without Nano Particle The calculated RMSF values for all atoms have been averaged to understand more details of the fluctuations of protein atoms (Table 8). The mean RMSF values in α-synuclein simulation in the presence of nanoparticles were higher compared to α-synuclein with no nanoparticles. Increasing RMSF values indicate a positive effect of nanoparticles on the instability of the α-synuclein molecule structure. α-synuclein simulations in the presence of P-CNT and BCN had the highest and lowest mean RMSF values during simulation, respectively. The effect of BCN has been positive in creating instability in the structure of α-synuclein, but less effective than other nanoparticles in creating instability in the molecular structure of α-synuclein. The most significant instability in the molecular structure of α-synuclein has been performed by P-CNT, which means that P-CNT is the best nanoparticle to prevent amyloid fibrillation.

Supplementary Files

This is a list of supplementary files associated with this preprint. Click to download.

- Figextra.JPG